ADVANCES IN APPLIED MECHANICS, VOLUME 33

Strain Gradient Plasticity

N. A. FLECK

Engineering Department, Cambridge University
Cambridge, England

and

J. W. HUTCHINSON

Division of Applied Sciences, Harvard University
Cambridge, MA

0065-2165/97 $25.00

I. Introduction

Dislocation theory suggests that the plastic flow strength of a solid depends on strain gradients in addition to strains. Hardening is due to the combined presence of geometrically necessary dislocations associated with a plastic strain gradient and statistically stored dislocations associated with plastic strain. In general, strain gradients are inversely proportional to the length scale over which plastic deformations occur. Thus, gradient effects become important for plastic deformations taking place at small scales. Experimental evidence suggests that flow strength increases with diminishing size, at length scales on the order of several microns or less. Phenomenological theories of strain gradient plasticity are proposed in this article as formulations which have either a deformation or flow theory character. The theories are intended for applications to materials and multilayers, both engineered and natural, whose dimensions controlling plastic deformation fall roughly within the range from a tenth of a micron to ten microns. Problems in this range of length scales generally have sufficiently large numbers of dislocations that a continuum approach is essential for quantitative modelling. At even smaller scales, problems tend to fall into the class where dislocations must be treated as discrete entities. At length scales above several microns, conventional plasticity theories which neglect gradient effects usually suffice.

The most general versions of the theories proposed here fit within the Toupin-Mindlin strain gradient framework, which involves all components of the strain gradient tensor and work-conjugate higher-order stresses in the form of couple stresses and double stresses. A specialized version deals with only a subset of the strain gradient tensor in the form of deformation curvatures (i.e., rotation gradients); this is the simpler couple stress framework. To motivate the entire approach, a survey of size-dependent phenomena in plasticity is presented early in the article in Section II. The phenomena are interpreted in terms of the phenomenological deformation theory of strain gradient plasticity. The review covers size effects noted in the torsion of thin wires, indentation tests, the macroscopic strengthening of metal matrix composites due to rigid particles, and the role of strain gradients in influencing both the growth of micron-sized voids and the stresses at the tip of a sharp crack. Emphasis in this review is on highlighting potential applications of strain gradient plasticity and on identifying possible experiments for validating and calibrating the theory. A strain gradient theory of single crystal plasticity is outlined in the final

section. Possible applications of the single-crystal theory are discussed, as are its implications for the phenomenological theories on which most of the developments in the article rest.

Experimental evidence is accruing for the existence of a strong size effect in the plastic flow of metals and ceramics. For example, the measured indentation hardness of metals and ceramics increases by a factor of about two as the width of the indent is decreased from about 10 μm to 1 μm as seen for one set of data in Figure 1 (Stelmashenko *et al.*, 1993; Ma and Clarke, 1995; Poole *et al.*, 1996). The scaled shear strength of copper wires in torsion in Figure 2(a) increases with diminishing wire diameter in the range 100 μm to 10 μm by almost a factor of three (Fleck *et al.*, 1994), while data for the uniaxial tensile behavior of the wires, for which gradients are absent, show essentially no size effect (see Figure 2(b)). The well-known Hall-Petch effect states that the yield strength of pure metals increases with diminishing grain size. Long-standing observations of shear bands in metals have revealed that micro-shear band widths appear to be consistently on the order of a micron. Simple dimen-

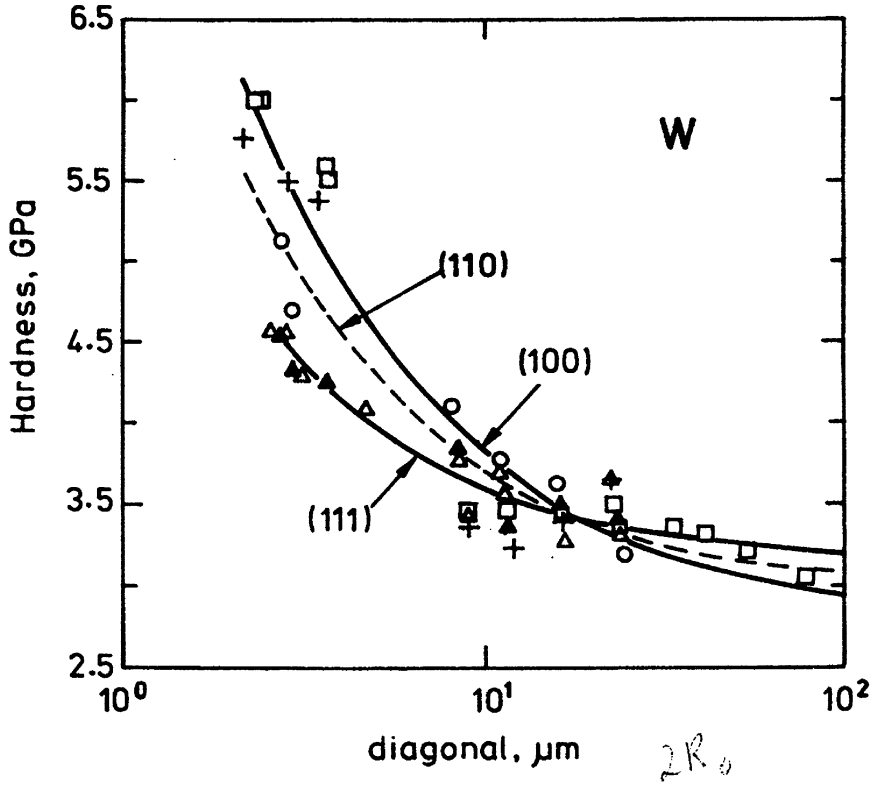

FIG. 1. Effect of indent size upon indentation hardness for tungsten single crystals (the data are taken from Stelmashenko *et al.*, 1993). The indent size is characterized by the diagonal of the indent from a Vickers micro-indenter (four-sided pyramid). A minor effect of crystal orientation on hardness is evident.

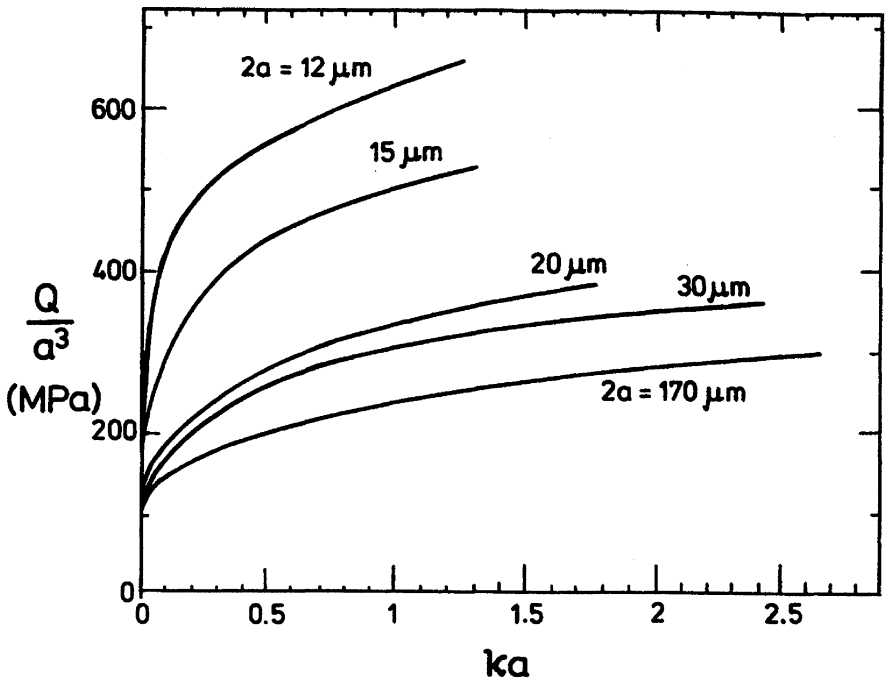

(a)

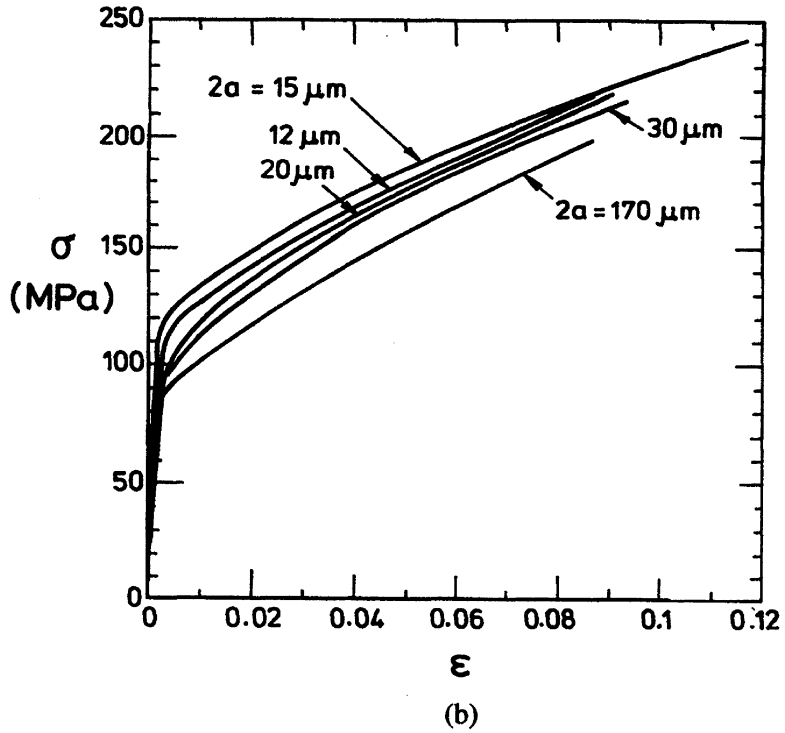

(b)

FIG. 2. a) Torsional response of copper wires of diameter $2a$ in the range 12 μm to 170 μm. Both the torque Q and the twist per unit length κ are scaled by the wire radius a. If the constitutive law were independent of strain gradients, the plots of normalized torque Q/a^3 versus κa would all lie on the same curve. b) True stress σ versus logarithmic strain ε tension data for copper wires of diameter $2a$ in the range 12 μm to 170 μm. There is a negligible effect of wire diameter on the behavior.

sional arguments lead to the conclusion that any continuum theory for each of these phenomena based solely on strain hardening, with no strain gradient dependence, would necessarily predict an absence of any such size effect.

In each of these cases it is thought that the size effect is associated with the presence of a large spatial gradient of strain which requires the storage of geometrically necessary dislocations, as discussed by Ashby (1970). The main physical arguments for a size effect within the context of continuum plasticity have already been presented by Fleck and Hutchinson (1993) and Fleck *et al.* (1994), and only a brief summary is presented here. The underlying idea is that material flow strength is controlled by the total density of dislocations which have been stored. Attention is directed to distributions of large numbers of dislocations, and not with individual dislocation interactions. Dislocations are stored for two reasons:

(i) In principle, a single crystal strained uniformly need not store dislocations, but dislocations do accumulate by random trapping. These are referred to as *statistically stored dislocations* or geometrically redundant dislocations (Ashby, 1970, 1971). As yet, there is no simple theory to predict the density ρ_S of these dislocations as a function of strain, though the dependence has been measured by numerous investigators (see, for example, Basinski and Basinski, 1966).

(ii) When a crystal is subjected to nearly any gradient of plastic strain, *geometrically necessary dislocations* must be stored. Plastic strain gradients appear either because of the geometry of the solid (e.g., near the tip of a crack) or because the material itself is plastically inhomogeneous (containing non-deforming phases, for instance). The density of the geometrically necessary dislocations can be calculated if the gradient of plastic slip on crystal planes is known, as is explained more fully in Section V below.

Consider examples in which each type of dislocation storage mechanism operates. First, in the uniaxial straining of a metallic single-crystal bar, plastic strain is macroscopically uniform and hardening is due to the random trapping of statistically stored dislocations. The dislocations are trapped as dipoles with short range stress fields. These dipoles act as a forest of sessile dislocations, and strain hardening is associated with the elevation of the macroscopic flow stress required to cut the dipoles by subsequent glide dislocations. Second, the plastic bending of an initially straight single-crystal beam to a macroscopic curvature κ requires the

storage of a uniform density $\rho_G = |\kappa|/\mathbf{b}$ of geometrically necessary edge dislocations, where $\mathbf{b}$ is the Burgers vector of the dislocations (Nye, 1953). One such dislocation distribution giving rise to the curvature is shown in Figure 3. Since $|\kappa|$ is the magnitude of the plastic gradient across of the height of the beam, ρ_G scales linearly with the imposed plastic-strain gradient. The density of these geometrically necessary dislocations can be measured directly via the lattice curvature (see Ashby, 1970; Russel and Ashby, 1970; Brown and Stobbs, 1976). These dislocations provide additional macroscopic strengthening caused by short-range interaction, e.g., when they are cut by glide dislocations a jog must be created. The energy barrier for jog formation shows up as an elevation in the macroscopic flow strength.

In order to define ρ_G precisely for the case of a single-slip system we assume that slip occurs in a direction s aligned with the x_1-axis, and the normal to the slip plane $\mathbf{m}$ is along the x_2 axis. Thus, the Burger's vector $\mathbf{b}$ of dislocations inducing the slip is co-directional with $\mathbf{s}$. A gradient of slip $\partial\gamma/\partial x_1$ gives rise to a density

$$\frac{1}{b}\frac{\partial\gamma}{\partial x_1}$$

of geometrically necessary edge dislocations lying along the $\mathbf{x}_3$-direction. Likewise, a gradient of slip $\partial\gamma/\partial x_3$ gives rise to a density

$$\frac{1}{b}\frac{\partial\gamma}{\partial x_3}$$

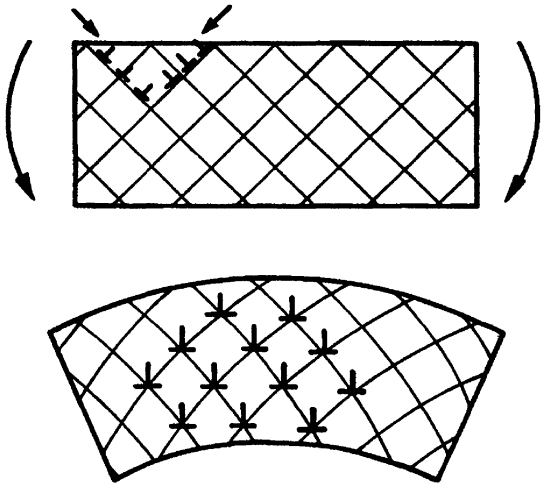

FIG. 3. Dislocation distribution in bending of a crystal with two symmetric slip systems. The density of geometrically necessary dislocations ρ_G is related to the curvature κ of the beam and to the magnitude of Burger's vector $\mathbf{b}$ by $\rho_G = |\kappa|/\mathbf{b}$.

of screw dislocations lying along the x_1 direction. Note that a slip gradient in the direction of the normal **m** to the slip plane requires no storage of dislocations.

It is assumed that the flow strength for a single-slip system of a single crystal depends upon the sum of the densities of statistically stored dislocations, ρ_S, and geometrically necessary dislocations, ρ_G. The simplest possible dimensionally correct relationship between the flow strength τ_y on the slip plane and total dislocation density is

$$\tau_y = CGb\sqrt{\rho_S + \rho_G} \tag{1.1}$$

where G is the shear modulus, b is the magnitude of the Burger's vector and C is a constant taken to be 0.3 by Ashby (1970). The contribution to flow strength from the Peierls-Nabarro or lattice-friction stress has been dropped from (1.1) as we shall focus on applications where strain hardening dominates material response. Other couplings between ρ_S and ρ_G are possible; equation (1.1) gives one particular form of the non-linear interaction between flow strength τ_y and dislocation densities ρ_S and ρ_G. Subsequently, this functional relationship will be modified in order to develop a phenomenological theory which fits more comfortably within the established general framework of plasticity theory.

To provide an article which is accessible to as wide a range of readers as possible, we have postponed the full development of strain gradient plasticity theory to Sections III and IV of the article. Section II, which follows, is intended as a self-contained review of the current status of strain gradient theory as it applies to a number of important plasticity phenomena at small scales. To begin the review, it is first necessary for us to specify precisely how the strains and strain gradients are introduced into the phenomenological constitutive models, but all other technical details of the theory are saved for later sections. A reader whose primary purpose is to acquire some acquaintance with the applicability of strain gradient plasticity may want to focus mainly on Section II.

II. Survey of Strain Gradient Plasticity: Formulations and Phenomena

Higher-order continuum theories of elasticity were promulgated in the 1960s culminating with the major contributions of Koiter (1964), Mindlin (1964, 1965) and Toupin (1962). Efforts were made to apply the theories to

predict phenomena for linear elastic solids such as stress concentration at holes (Mindlin, 1963), crack-tip stresses (Eringen, 1968; Sternberg and Muki, 1967), bending stiffness of thin beams (Koiter, 1964), and stresses at free surfaces (Mindlin, 1965). No experimental corroboration of these theories was achieved, and in due course it was generally accepted that the phenomena being addressed in these works should be expected to come into play only at scales comparable to atomic lattice spacing. Specifically, Koiter's (1964) argument prevailed to the effect that there is no reason to expect gradient effects to alter the elastic bending stiffness of a single crystal beam until its thickness approaches atomic dimensions.

Higher-order effects can be expected to come into play in conventional linear elastic solids when the representative length scale L of the deformation field becomes comparable to a micro-structural length scale (Mindlin, 1964). As an example, a higher-order approach has been applied to the propagation of waves through layered media (Sun *et al.*, 1968). When the wavelength is very long compared to the thickness of the layers, conventional theory using appropriate composite averages of the layer moduli and densities can be used to describe the wave. However, for wavelengths which begin to approach the thickness of the layers, higher-order theories have been derived bringing in the effects of strain gradients on wave behavior. Similarly, polycrystalline solids with anisotropic grains or elastic solids reinforced by a population of stiff particles can be expected to display behaviors which depart from predictions of conventional elasticity theory based on the concept of composite moduli when the characteristic length scale of the overall deformation field L begins to approach the grain size or particle spacing. There have been several studies directed to such problems with the aim of providing higher-order strain gradient constitutive relations for conventional linear elastic solids with micro-structure (e.g., Zuiker and Dvorak, 1994; Drugan and Willis, 1996 for materials reinforced by spherical particles, and Bardenhagen and Triantafyllidis, 1996 for multi-phase media). Complementing this theoretical work are the experiments by Kakunai *et al.* (1985) on polycrystalline aluminium beams with equiaxed grains showing a small but systematic increase in the scaled elastic-bending stiffness as the thickness of the beams is reduced from about sixty to three grain diameters.

While gradient effects in an elastic single crystal of pure metal become significant only for deformation fields with wavelengths on the order of the atomic spacing, when plastic deformation occurs, gradient effects can become important at much larger scales. Examples displaying size effects

in the micron range are seen in Figures 1 and 2. The larger scales in the plastic range are fundamentally related to dislocation cell micro-structures which develop with dimensions on the order of sub-microns. Other problems to be discussed below are the plastic flow strength of particle reinforced metal-matrix composites, where size effects are expected to become important at micron particle spacings, and the grain size dependence of yielding in a polycrystal when the grain diameters are in this same range. In all of these cases, the representative length scale L of the deformation field sets the magnitude of plastic strain gradients compared with the magnitude of the average plastic strains. A small representative length scale implies the presence of large strain gradients relative to strains, and, consequently, a large density of geometrically necessary dislocations relative to statistically stored dislocations.

A large body of literature has emerged on the development of non-local theories for addressing the localization of deformation in dilatant plastic solids, such as granular materials. In early work it was assumed that the solid deforms as a Cosserat continuum, whereby the strength depends upon both strain and the material curvature (Muhlhaus, 1985, 1989; de Borst, 1993). The Cosserat theory has been extended by Steinmann (1994) to finite strain; the resulting formulation is complex, largely due to the problem of defining rotation and curvature at finite deformation. A plasticity version of the Cosserat approach is developed further in Section A below. It has been recognized that Cosserat theory has little effect on the stress state during localization in a dilatant plastic solid, as curvatures are small within the dilating band of concentrated deformation. An alternative gradient theory has proved popular under these circumstances: this theory invokes strengthening by the first and second Laplacian of effective strain (Aifantis, 1984; Zbib and Aifantis, 1989; Muhlhaus and Aifantis, 1991). The emphasis has been placed on developing robust numerical procedures for prediction of the width of a localized band of deformation, and developments of the theory have been to include dynamic effects (Sluys *et al.*, 1993). It is recalled that conventional constitutive descriptions give a pathological mesh-size dependence upon localization of deformation.

Under general loading histories, plasticity is intrinsically a path-dependent phenomenon requiring a non-integrable description which relates increments of stress-like quantities to increments of strain-like quantities. Such constitutive theories are referred to collectively as *flow theories*. Because of their simpler nature, deformation theories of plasticity have occupied a prominent position in the development of phenomenolog-

ical constitutive models. These are generally small strain, nonlinear elastic constitutive models whose functional form is chosen to reproduce a representative stress history, such as uniaxial tension, and to be in accord with selected physical constraints such as incompressibility of plastic flow. Application of deformation theories is necessarily limited to problems where path-dependence is not an issue. It is well known, for example, that predictions of J_2 deformation theory coincide with those of J_2 flow theory for all histories where the stress components increase proportionally (Budiansky, 1959). None of the problems in the survey which follows has any important path-dependent behavior, and, therefore, we will discuss and analyze them within the context of the deformation theories of strain-gradient plasticity. In addition, large strain effects are not the dominant feature in any of the problems, and thus the discussion can be further simplified by restricting attention to small strain deformation theories.

A. Rotation Gradients: Couple Stress Theory

Fleck and Hutchinson (1993) have developed a phenomenological theory of strain gradient plasticity based on gradients of rotation which fits with the framework of couple stress theory. This theory is probably the simplest generalization of conventional isotropic-hardening plasticity theory to include strain gradient effects. For this reason, we begin by specifying the strain and strain gradient invariants characterizing the deformation theory version of this constitutive law. Full details of the flow theory version are spelled out in Section IV.

The yield strength of the solid is taken to depend upon both strain ε and curvature χ. The small strain assumption is adopted, and a Cartesian reference frame x_i is employed. The strain tensor $\boldsymbol{\varepsilon}$ is related to the material displacement $\mathbf{u}$ via $\varepsilon_{ij} = (u_{i,j} + u_{j,i})/2$, and the curvature $\boldsymbol{\chi}$ is the spatial gradient of the material rotation $\boldsymbol{\theta}$:

$$\chi_{ip} = \theta_{i,p} = \frac{1}{2} e_{ijk} u_{k,jp} = e_{ijk} \varepsilon_{kp,j} \tag{2.1}$$

(Unless otherwise stated, the usual summation convention applies for repeated indices.) In the deformation theory version of the theory, the strain energy density w of an incompressible solid is taken to depend upon the second, von Mises invariant of strain, $\varepsilon_e = \sqrt{\frac{2}{3}\varepsilon_{ij}\varepsilon_{ij}}$, and the analo-

gous second invariant of the curvature, $\chi_e = \sqrt{\frac{2}{3}\chi_{ij}\chi_{ij}}$. For the sake of simplicity, Fleck and Hutchinson (1993) neglected any dependence of w upon the other quadratic invariant of χ given by $\sqrt{\frac{2}{3}\chi_{ij}\chi_{ji}}$. Further, they assumed that w depends only upon the 'overall effective strain' quantity $\mathscr{E}_{CS}$ where

$$\mathscr{E}_{CS} = \sqrt{\varepsilon_e^2 + \ell_{CS}^2 \chi_e^2} \tag{2.2}$$

Here, the material length scale ℓ_{CS} has been introduced as required for dimensional consistency, and the subscript '*CS*' is short for 'couple stress' to avoid confusion with other material length scales introduced later.

To assess the sensitivity of predictions to the way in which ε_e and χ_e are combined in forming $\mathscr{E}_{CS}$, solutions will be presented to several problems using the following generalization of (2.2):

$$\mathscr{E}_{CS} = [\varepsilon_e^\mu + \ell_{CS}^\mu \chi_e^\mu]^{1/\mu} \tag{2.3}$$

where an additional parameter μ has been introduced. There is some rationale for assuming $\mu = 1$, based on the following dislocation arguments. Assume that the flow strength depends upon the total dislocation density $\rho_T = \rho_S + \rho_G$, and that ρ_G is linear in the strain gradient as discussed in Section I. If one further assumes that the density of statistically stored dislocations ρ_S is linear in von Mises effective strain (stage I hardening for a single crystal response), then one concludes that an appropriate scalar measure of hardening is given by (2.3) with $\mu = 1$. A value for μ equal to 2 is more attractive on mathematical grounds and can be rationalized by assuming densities of statistically stored and geometrically necessary dislocations interact such that the total dislocation density ρ_T is the harmonic sum of ρ_S and ρ_G, i.e. $\rho_T^2 = \rho_S^2 + \rho_G^2$.

B. Rotation and Stretch Gradients: Toupin-Mindlin Theory

Couple stress theory is a subset of a more general isotropic-hardening theory based on all the quadratic invariants of the strain gradients. The extended theory assumes a dependence on stretch gradients as well as rotation gradients and fits within the more general framework as laid down by Toupin (1962) and Mindlin (1964, 1965). Leroy and Molinari (1993) have extended this framework to include the effects of finite strains.

The generalized strain variables are the symmetric strain tensor $\varepsilon_{ij} = \frac{1}{2}(u_{i,j} + u_{j,i})$ and the second gradient of displacement $\eta_{ijk} \equiv \bar{\partial}_i \bar{\partial}_j u_k = u_{k,ij}$, where $\bar{\partial}_i$ is the forward gradient operator. The work increment per unit volume of solid due to an arbitrary variation of displacement $\mathbf{u}$ is

$$\delta w = \sigma_{ij}\, \delta\varepsilon_{ij} + \tau_{ijk}\, \delta\eta_{ijk} \tag{2.4}$$

where the symmetric Cauchy stress σ_{ij} is the work conjugate of the strain variation $\delta\varepsilon_{ij}$ and the higher-order stress τ_{ijk} $(= \tau_{jik})$ is the work conjugate of the strain gradient variation $\delta\eta_{ijk}$. The higher-order stress tensor is composed of components of both couple stresses and double stresses as will be displayed explicitly in Section III.

A phenomenological isotropic deformation theory version of plasticity is now developed for the case where the strain energy density w depends upon both the second-order symmetric strain tensor $\boldsymbol{\varepsilon}$ and the third-order strain gradient tensor $\boldsymbol{\eta}$. The work statement (2.4) implies that the second-order symmetric stress $\boldsymbol{\sigma}$ is given by $\sigma_{ij} = \partial w / \delta\varepsilon_{ij}$ and the third-order stress $\boldsymbol{\tau}$ is given by $\tau_{ijk} = \partial w / \partial\eta_{ijk}$. Toupin (1962) and Mindlin (1965) considered a general linear isotropic hyper-elastic solid. They showed that the strain energy density w depends upon $\boldsymbol{\varepsilon}$ and $\boldsymbol{\eta}$ in the manner

$$w = \frac{1}{2}\lambda\varepsilon_{ii}\varepsilon_{jj} + \mu\varepsilon_{ij}\varepsilon_{ij} + a_1\eta_{ijj}\eta_{ikk} + a_2\eta_{iik}\eta_{kjj} + a_3\eta_{iik}\eta_{jjk} + a_4\eta_{ijk}\eta_{ijk} + a_5\eta_{ijk}\eta_{kji} \tag{2.5}$$

where the constants λ and μ are the standard Lamé constants and the five a_n are additional stiffness constants of dimension stress times length squared. For the special case of an incompressible solid ε_{ii} and η_{ijj} vanish, and the above expression for w simplifies to

$$w = \mu\varepsilon'_{ij}\varepsilon'_{ij} + a_3\eta'_{iik}\eta'_{jjk} + a_4\eta'_{ijk}\eta'_{ijk} + a_5\eta'_{ijk}\eta'_{kji} \tag{2.6}$$

where the superscript $(')$ is introduced to emphasize that the strain quantities are derived from an incompressible displacement field. We shall specify the hydrostatic part $\boldsymbol{\eta}^H$ of $\boldsymbol{\eta}$ to be

$$\eta^H_{ijk} \equiv \frac{1}{4}(\delta_{ik}\eta_{jpp} + \delta_{jk}\eta_{ipp}) \tag{2.7}$$

so that $\eta^H_{ijk} = \eta^H_{jik}$ and $\eta^H_{ijj} = \eta_{ijj}$. The deviatoric part of $\boldsymbol{\eta}$ follows as $\boldsymbol{\eta}' = \boldsymbol{\eta} - \boldsymbol{\eta}^H$. Note that $\boldsymbol{\eta}'$ is orthogonal to any arbitrary hydrostatic displacement field $\tilde{\boldsymbol{\eta}}^H$ such that $\boldsymbol{\eta}' : \tilde{\boldsymbol{\eta}}^H = 0$.

Now consider the more general case of an incompressible isotropic non-linear deformation theory solid. Following the strategy of Fleck and Hutchinson (1993), the strain energy density w for a *non-linear elastic solid* is assumed to be a non-linear function of the combined strain quantity $\mathscr{E}$ where

$$\mathscr{E}^2 = \frac{2}{3}\varepsilon'_{ij}\varepsilon'_{ij} + c_1\eta'_{iik}\eta'_{jjk} + c_2\eta'_{ijk}\eta'_{ijk} + c_3\eta'_{ijk}\eta'_{kji} \tag{2.8}$$

The factor of $2/3$ pre-multiplies the $\varepsilon'_{ij}\varepsilon'_{ij}$ invariant so that $\mathscr{E}$ equals the von Mises strain invariant ε_e in the case of uniform strain. The precise dependence of w on $\mathscr{E}$, and the values of the three factors c_n remain to be specified. It is convenient at this stage to re-express $\boldsymbol{\eta}'$ in terms of a unique orthogonal decomposition introduced by Smyshlyaev and Fleck (1996). They have shown that $\boldsymbol{\eta}'$ may be written as

$$\boldsymbol{\eta}' = \boldsymbol{\eta}'^{(1)} + \boldsymbol{\eta}'^{(2)} + \boldsymbol{\eta}'^{(3)} \tag{2.9}$$

where $\boldsymbol{\eta}'^{(i)} : \boldsymbol{\eta}'^{(j)} = 0$ for $i \neq j$. The three parts $\boldsymbol{\eta}'^{(i)}$ are defined as follows. First, introduce the fully symmetric tensor $\boldsymbol{\eta}'^{S}$ where

$$\eta'^{S}_{ijk} = \frac{1}{3}[\eta'_{ijk} + \eta'_{jki} + \eta'_{kij}] \tag{2.10}$$

Note that η'^{S} has the symmetries $\eta'^{S}_{ijk} = \eta'^{S}_{jki} = \eta'^{S}_{kij}$ in addition to the symmetry in the first two indices $\eta'^{S}_{ijk} = \eta'^{S}_{jik}$. The symmetric triad η'^{S} has ten independent components. The eight components of the remainder $\boldsymbol{\eta}'^{A} \equiv \boldsymbol{\eta}' - \boldsymbol{\eta}'^{S}$ can be specified in terms of the deviatoric part of the curvature tensor $\chi'_{ij} = \theta'_{i,j} = \frac{1}{2}e_{iqr}\eta'_{jqr}$ as follows:

$$\eta'^{A}_{ijk} \equiv \eta'_{ijk} - \eta'^{S}_{ijk} = \frac{2}{3}e_{ikp}\chi'_{pj} + \frac{2}{3}e_{jkp}\chi'_{pi} \tag{2.11}$$

Note that the decomposition of $\boldsymbol{\eta}'$ into the parts $\boldsymbol{\eta}'^{S}$ and $\boldsymbol{\eta}'^{A}$ is an orthogonal decomposition, i.e., $\eta'^{S}_{ijk}\eta'^{A}_{ijk} = 0$.

The orthogonal decomposition of $\boldsymbol{\eta}'$ into the three tensors $\boldsymbol{\eta}'^{(i)}$ is given by

$$\eta'^{(1)}_{ijk} = \eta'^{S}_{ijk} - \frac{1}{5}\left[\delta_{ij}\eta'^{S}_{kpp} + \delta_{jk}\eta'^{S}_{ipp} + \delta_{ki}\eta'^{S}_{jpp}\right] \tag{2.12}$$

$$\eta'^{(2)}_{ijk} = \frac{1}{6}[e_{ikp}e_{jlm}\eta'_{lpm} + e_{jkp}e_{ilm}\eta'_{lpm} + 2\eta'_{ijk} - \eta'_{jki} - \eta'_{kij}] \tag{2.13}$$

$$\eta'^{(3)}_{ijk} = \frac{1}{6}[-e_{ikp}e_{jlm}\eta'_{lpm} - e_{jkp}e_{ilm}\eta'_{lpm} + 2\eta'_{ijk} - \eta'_{jki} - \eta'_{kij}]$$

$$+ \frac{1}{5}[\delta_{ij}\eta'^{S}_{kpp} + \delta_{jk}\eta'^{S}_{ipp} + \delta_{ki}\eta'^{S}_{jpp}] \tag{2.14}$$

Note that each of the three quantities $\boldsymbol{\eta}'^{(i)}$ possess the symmetry $\eta'^{(n)}_{ijk} = \eta'^{(n)}_{jik}$ and satisfies the incompressibility constraint that $\eta'^{(n)}_{ijj}$ vanishes.

The combined strain quantity $\mathscr{E}$ can be written in terms of $\boldsymbol{\varepsilon}'$ and $\boldsymbol{\eta}'^{(i)}$ by making use of (2.12–2.14) to get, after somewhat lengthy manipulation,

$$\mathscr{E}^2 = \frac{2}{3}\varepsilon'_{ij}\varepsilon'_{ij} + \ell_1^2\eta'^{(1)}_{ijk}\eta'^{(1)}_{ijk} + \ell_2^2\eta'^{(2)}_{ijk}\eta'^{(2)}_{ijk} + \ell_3^2\eta'^{(3)}_{ijk}\eta'^{(3)}_{ijk} \tag{2.15}$$

where

$$\ell_1^2 = c_2 + c_3, \quad \ell_2^2 = c_2 - \frac{1}{2}c_3 \quad \text{and} \quad \ell_3^2 = \frac{5}{2}c_1 + c_2 - \frac{1}{4}c_3 \tag{2.16}$$

We shall take (2.15) to be the defining relation for $\mathscr{E}$. Note that (2.15) ensures that $\mathscr{E}$ is convex in the strain quantities $(\boldsymbol{\varepsilon}', \boldsymbol{\eta}')$.

The connection between the general first-order strain gradient theory involving the three invariants of $\boldsymbol{\eta}'^{(i)}$ given in (2.15) and couple stress theory may be stated as follows. In couple stress theory the two curvature invariants are $\chi'_{ij}\chi'_{ij}$ and $\chi'_{ij}\chi'_{ji}$. These invariants may be re-expressed in terms of $\boldsymbol{\eta}'^{(i)}$ via (2.1) and (2.12–2.14) to give

$$\chi'_{ij}\chi'_{ij} = \frac{3}{8}\eta'^{(2)}_{ijk}\eta'^{(2)}_{ijk} + \frac{5}{16}\eta'^{(3)}_{ijk}\eta'^{(3)}_{ijk} \tag{2.17}$$

and

$$\chi'_{ij}\chi'_{ji} = \frac{3}{8}\eta'^{(2)}_{ijk}\eta'^{(2)}_{ijk} - \frac{5}{16}\eta'^{(3)}_{ijk}\eta'^{(3)}_{ijk} \tag{2.18}$$

These relations may be inverted to allow us to write

$$\eta'^{(2)}_{ijk}\eta'^{(2)}_{ijk} = \frac{4}{3}\chi'_{ij}\chi'_{ij} + \frac{4}{3}\chi'_{ij}\chi'_{ji}$$

and $\eta'^{(3)}_{ijk}\eta'^{(3)}_{ijk} = \frac{8}{5}\chi'_{ij}\chi'_{ij} - \frac{8}{5}\chi'_{ij}\chi'_{ji}$, and thus $\mathscr{E}$ in (2.15) can be rewritten in terms of the three invariants $\chi'_{ij}\chi'_{ij}$, $\chi'_{ij}\chi'_{ji}$ and $\eta'^{(1)}_{ijk}\eta'^{(1)}_{ijk}$ as

$$\mathscr{E}^2 = \frac{2}{3}\varepsilon'_{ij}\varepsilon'_{ij} + \ell_1^2\eta'^{(1)}_{ijk}\eta'^{(1)}_{ijk} + \left(\frac{4}{3}\ell_2^2 + \frac{8}{5}\ell_3^2\right)\chi'_{ij}\chi'_{ij} + \left(\frac{4}{3}\ell_2^2 - \frac{8}{5}\ell_3^2\right)\chi'_{ij}\chi'_{ji}. \tag{2.19}$$

It is now readily apparent that the Fleck–Hutchinson couple stress theory is a special case of (2.19) where the only non-vanishing strain gradient contribution to $\mathscr{E}$ is the curvature invariant $\chi'_{ij}\chi'_{ij}$. Formally, (2.19) may

be reduced to the couple stress version (2.2) by taking $\ell_1 = 0$, $\ell_2 = \frac{1}{2}\ell_{CS}$ and $\ell_3 = \sqrt{\frac{5}{24}}\,\ell_{CS}$.

In the sequel, results will be presented for a number of problems for both the special case of the couple stress solid (denoted by CS) and the more general solid which is dependent on both stretch and rotation gradients (denoted by SG). Specifically, results will be given for the following two solids:

$$\begin{aligned} &\text{CS:} \quad \ell_1 = 0, \quad \ell_2 = \frac{1}{2}\ell, \quad \ell_3 = \sqrt{\frac{5}{24}}\,\ell \quad \text{where } \ell \equiv \ell_{CS} \\ &\text{SG:} \quad \ell_1 = \ell, \quad \ell_2 = \frac{1}{2}\ell, \quad \ell_3 = \sqrt{\frac{5}{24}}\,\ell \end{aligned} \tag{2.20}$$

This brings the notation for the CS solid into coincidence with that used in the two earlier papers by Fleck and Hutchinson (1993) and Fleck *et al.* (1994) Neither of these two solids has a dependence on the second rotation invariant, $\chi'_{ij}\chi'_{ji}$, but the effect of this invariant appears to be relatively unimportant in each case we have investigated.

The above general strain gradient theory will be used in the remainder of this section to predict material-based size effects in a number of applications. For simplicity, a power law dependence of the strain energy density w on the effective strain $\mathscr{E}$ will be assumed of the form

$$w = \frac{n}{n+1}\Sigma_0 \mathscr{E}_0 \left(\frac{\mathscr{E}}{\mathscr{E}_0}\right)^{(n+1)/n} \tag{2.21}$$

where Σ_0, $\mathscr{E}_0$ and the strain-hardening exponent n are taken to be material constants. For the case of uniaxial tension the uniaxial stress σ is related to the axial strain ε by the familiar expression

$$\sigma = \Sigma_0 \left(\frac{\varepsilon}{\mathscr{E}_0}\right)^{1/n}.$$

Additional details on the deformation theory above are given in the Appendix; the flow theory version is explained in Section IV.

C. Phenomena Influenced by Plastic Strain Gradients

1. *Torsion of Thin Wires*

Fleck *et al.* (1994) performed tension experiments and torsion experiments on pure copper wires whose diameters ranged from 12 μm to 170 μm. The results are summarized in Figure 2. They observed a strong size

effect in torsion whereby the shear flow strength of the thinnest wires was about three times that of the thickest wires. No size effects were observed in the tension tests which produce no strain gradients. For each wire of radius a, a power law relation between torque Q and the associated twist per unit length κ of the wire:

$$\frac{Q}{a^3} = k(\kappa a)^{1/n} \tag{2.22}$$

gave a good fit to the experimental data. The strain-hardening index was measured to be $n \cong 5$ independent of wire radius, and the constant of proportionality k was observed to increase with diminishing wire radius a. Note that the non-dimensional group κa may be interpreted as the magnitude of the shear strain at the surface of the wire, and the normalized torque Q/a^3 is a measure of the shear stress across the specimen in some averaged sense. The observation that k depends on wire radius implies that the constitutive law for the copper must contain a material length scale. To see this, consider the counter argument. If the local shear stress at any point in the wire were to depend only upon shear strain independent of any material length quantity, then it is straightforward to show by dimensional analysis that the curves of Q/a^3 versus κa must superimpose. Clearly they don't. Inclusion of strain gradients in the constitutive law necessarily introduces a material length scale ℓ which gives rise to a dependence of k on a/ℓ, and we proceed to investigate the quantitative implications of doing so.

Fleck *et al.* (1994) matched the predictions of their couple stress version of strain gradient theory (given by (2.2) and (2.21)) to the observed torsional response of the copper wires by selecting a value for the length scale ℓ_{CS} equal to 3.7 μm. The following questions now arise:

(i) Is the predicted torsional response for the more general strain gradient theory given by (2.15) and (2.21) different from the special case of couple stress theory?

(ii) Is the predicted response sensitive to the nature of the functional form assumed for the overall strain measure $\mathscr{E}$ in terms of the strain invariants $\varepsilon'_{ij}\varepsilon'_{ij}$, $\eta'^{(1)}_{ijk}\eta'^{(1)}_{ijk}$, $\eta'^{(2)}_{ijk}\eta'^{(2)}_{ijk}$ and $\eta'^{(3)}_{ijk}\eta'^{(3)}_{ijk}$? As illustrated by (2.3), the relation (2.15) gives only one particular choice of coupling the strains and strain gradients.

In answer to the first question, it can be noted that the invariants $\eta'^{(1)}_{ijk}\eta'^{(1)}_{ijk}$ and $\eta'^{(3)}_{ijk}\eta'^{(3)}_{ijk}$ vanish when evaluated using the torsional displacement field. The remaining strain gradient invariant, $\eta'^{(2)}_{ijk}\eta'^{(2)}_{ijk}$, can be

expressed in terms of $\chi'_{ij}\chi'_{ij}$ as $\eta'^{(2)}_{ijk}\eta'^{(2)}_{ijk} = \frac{4}{3}\chi'_{ij}\chi'_{ij}$. Thus, the more general theory involving three invariants of the strain gradient tensor is identically equivalent to the couple stress version for this problem upon taking $\ell_2 = (1/\sqrt{2})\ell_{CS}$.

In order to address the second question, the overall strain measure $\mathscr{E}$ is written in the more general form analogous to (2.3):

$$\mathscr{E} = \left[\left(\frac{2}{3}\varepsilon'_{ij}\varepsilon'_{ij}\right)^{\mu/2} + \left(\ell_1^2\eta'^{(1)}_{ijk}\eta'^{(1)}_{ijk}\right)^{\mu/2} + \left(\ell_2^2\eta'^{(2)}_{ijk}\eta'^{(2)}_{ijk}\right)^{\mu/2} + \left(\ell_3^2\eta'^{(3)}_{ijk}\eta'^{(3)}_{ijk}\right)^{\mu/2}\right]^{1/\mu} \tag{2.23}$$

where the range of the coupling coefficient μ is from 1 to 2, in accord with the rationale discussed earlier. The expression (2.23) for $\mathscr{E}$ is homogeneous and of degree one in the strain and strain gradient quantities, and reduces to (2.15) upon taking $\mu = 2$.

The relation between the torque Q and the twist per unit length κ of a wire modelled by the deformation theory solid (2.21) with (2.23) is deduced most simply by noting that the strain energy for a unit length of the bar is given by

$$\int_V w(\mathscr{E})\, dV = \int_0^\kappa Q(\kappa)\, d\kappa \tag{2.24}$$

Since Q is of degree $1/n$ in κ, (2.24) may be rewritten as

$$\int_V w(\mathscr{E})\, dV = \frac{n}{n+1} Q\kappa \tag{2.25}$$

Now, if (2.21) for w is expressed in terms of κ using the relation between the linear strain distribution across the wire and the twist and is then substituted into the left-hand side of (2.25) and integrated, one finds (with $\ell \equiv \ell_{CS}$)

$$\frac{Q}{a^3} = 2\pi\Sigma_0\left(\frac{\kappa a}{\mathscr{E}_0}\right)^{1/n}\left(\frac{\ell}{a}\right)^{(n+1)/n}\int_0^1\left[\xi\left(\left(\frac{\xi a}{\sqrt{3}\,\ell}\right)^{\mu} + 1\right)^{(n+1)/n\mu}\right]d\xi \tag{2.26}$$

In the limit classical limit, $\ell = 0$, the torque Q_0 follows from (2.26) as

$$Q_0 = \frac{2\pi}{\sqrt{3}}\,\frac{n}{3n+1}\,\Sigma_0 a^3\left(\frac{\kappa a}{\sqrt{3}\,\mathscr{E}_0}\right)^{1/n} \tag{2.27}$$

Integration of (2.26) can be done explicitly for $\mu = 1$ and $\mu = 2$, and the non-dimensional ratio Q/Q_0 reflecting the torque elevation due to strain gradient effects at the same κ is found to be

$$\frac{Q}{Q_0} = [1 + (\sqrt{3}\ell/a)]^{(3n+1)/n} - \frac{3n+1}{2n+1}(\sqrt{3}\ell/a)(1 + \sqrt{3}\ell/a)^{(2n+1)/n} + \frac{n}{2n+1}(\sqrt{3}\ell/a)^{(3n+1)/n} \quad (2.28)$$

for $\mu = 1$ and

$$\frac{Q}{Q_0} = \left[1 + (\sqrt{3}\ell/a)^2\right]^{(3n+1)/2n} - (\sqrt{3}\ell/a)^{(3n+1)/n} \quad (2.29)$$

for $\mu = 2$.

The non-dimensional torque ratio is plotted as a function of ℓ/a in Figure 4, for $\mu = 1$ and 2, and $n = 3$ and 5. For all cases shown there is a significant enhancement in torque by a factor of 3 to 5 when ℓ/a is increased from zero to unity. We further note that the elevation in torque

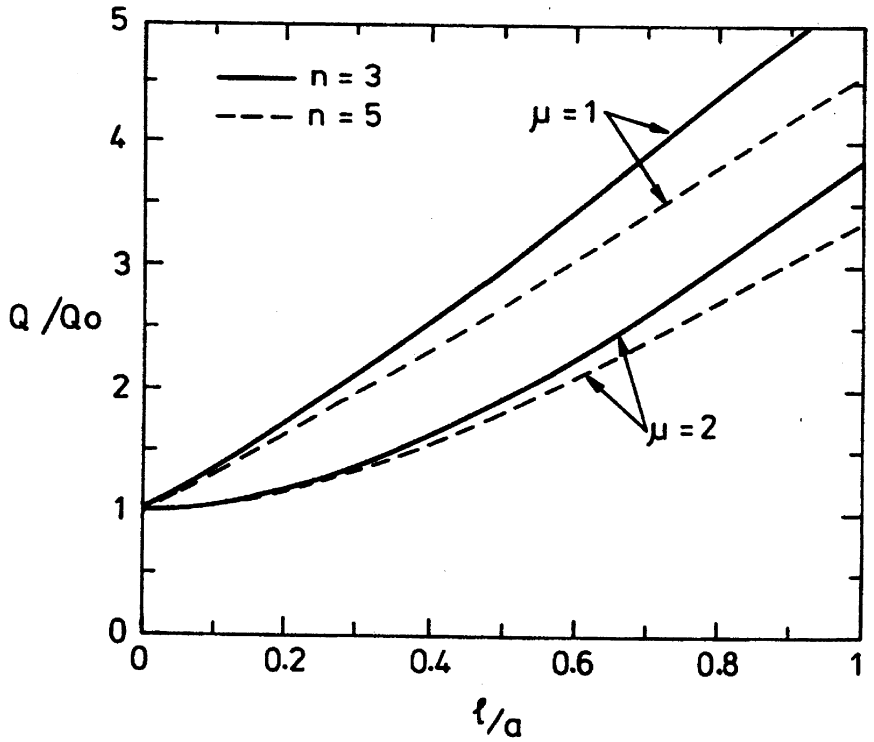

FIG. 4. Elevation in torsional strength due to strain gradients. The wire is of radius a and the torque Q at a given twist is normalized by the torque Q_0 required to achieve the same twist for a conventional solid.

with increasing ℓ/a is greater for $\mu = 1$ than for $\mu = 2$, and is greater for $n = 3$ than for $n = 5$.

At small values of ℓ/a, a greater size effect is shown for $\mu = 1$ than for $\mu = 2$. This is made explicit by the asymptotic expressions for Q/Q_0 at small ℓ/a. For $\mu = 1$, Q/Q_0 increases linearly with ℓ/a according to

$$\frac{Q}{Q_0} = 1 + \frac{(3n + 1)(n + 1)}{n(2n + 1)}(\sqrt{3}\,\ell/a) + O(\ell^2) \tag{2.30}$$

whereas for $\mu = 2$. Q/Q_0 increases quadratically with ℓ/a according to

$$\frac{Q}{Q_0} = 1 + \frac{3}{2}\frac{(3n + 1)}{n}(\ell/a)^2 + O(\ell^3) \tag{2.31}$$

The measured torsional response shown in Figure 2(a) may be used to deduce a value for the material length scale ℓ. Follow the same procedure as outlined by Fleck *et al.* (1994), we find that the magnitude of ℓ is somewhat sensitive to the value adopted for μ. For the case $\mu = 2$, $\ell \approx 4$ μm fits the data, while for $\mu = 1$, $\ell \approx 2$ μm. The value $\mu = 2$ will be used in most of the examples in the sequel as this value allows for a more robust numerical implementation of solution procedures in more complicated problems than is the case when $\mu = 1$. Nevertheless, the option of using (2.23) with a value such as $\mu = 1$ should not be foreclosed in constitutive modelling in the future, as the linear combination of strains and strain gradient terms may reproduce behavior better than the harmonic sum of these terms. Gradient contributions become numerically larger at smaller values of the gradient invariants relative to the strain invariants for the linear combination than for the harmonic sum, and this difference may be physically significant as suggested by (1.1). Indeed, the distinct differences in the elevation of the torque between $\mu = 1$ and 2 in the range of small ℓ/a which is evident in Figure 4 and in (2.30) and (2.31) may provide an opportunity to establish the choice by direct comparison with experimental data.

2. *The Grain Size Effect on Polycrystalline Yield Strength*

Ashby (1970) has argued that the grain size dependence of flow strength can be explained in terms of the anisotropy of slip from grain to grain. Consider a pure polycrystalline metal under uniaxial tension. If each grain were unconstrained to deform freely under the applied stress then any chosen grain would deform to a different shape from that of its neighbors due to the difference in its crystallographic orientation. To ensure compat-

ibility of deformation from grain to grain, the strain state within each grain is non-uniform, and geometrically necessary dislocations are generated within each grain in order for them to fit together. The simplest physical arguments reveal that the density ρ_G of the geometrically necessary dislocations scales with the average strain in each grain divided by the grain size d. (Measurements of dislocation densities in deformed polycrystals do seem to follow this law: the density increases linearly with tensile strain, and, at a given strain, the density scales with the reciprocal of the grain size. See for example Essmann *et al.*, 1968; McLean, 1967). For small grains the density ρ_G will exceed that of the statistically stored dislocations ρ_S, and relation (1.1) suggests that the elevation in flow strength scales with $d^{-1/2}$. This is consistent with the observed Hall-Petch grain-size relationship, whereby the elevation in yield strength due to grain-boundary strengthening varies as $d^{-1/2}$. We note in passing that Nix has shown that the grain-size effect on strength is enhanced when the material exists in the form of a thin layer on an elastic substrate (Nix, 1988).

A crystal plasticity version of the strain gradient theory is introduced in Section V below and can be used to explore the grain size effect in quantitative detail. Smyshlyaev and Fleck (1996) have used the linear limit of this crystal theory to predict the effect of grain size d on the macroscopic shear modulus of incompressible face-centered cubic (fcc) polycrystals. The linear result provides a useful qualitative guide to the effect of grain-size strengthening of non-linear polycrystals. Also, the linear result is the first step in the estimation of the grain-size effect for non-linear polycrystals: in order to use the non-linear variational principle of Ponte Castenada (1991, 1992) the effective properties of the linear solid are required.

In the linear analysis of Smyshlyaev and Fleck (1996) the crystals are oriented in a uniform manner, so that the macroscopic response of the polycrystal is isotropic and can be described by a single shear modulus μ^*. It is assumed that each fcc crystal contains 12 independent slip systems, and that each slip system deforms in shear with an associated shear modulus μ. The strain energy density W for each slip system is expressed in terms of both the elastic shear strain γ and the spatial gradient of shear strain $\nabla\gamma$ according to the assumed relation

$$W = \frac{1}{2}\mu\left[\gamma^2 + \ell^2|\nabla\gamma|^2\right] \tag{2.32}$$

where the material length scale ℓ ensures dimensional consistency. Hashin-Shtrikman bounds on the macroscopic shear modulus are shown in

Figure 5 as a function of the grain size d. It is found that the macroscopic stiffening varies approximately as $d^{-1/2}$, in support of the Hall-Petch relationship. However, the effect is not a strong one: as ℓ/d is increased from zero to unity, the macroscopic shear modulus increases by about 10%. It is well known that a strong Hall-Petch effect is not observed in fcc polycrystals due to the availability of a large number of slip systems for each crystal. Further calculations are required to determine the predicted grain-size effect for non-linear fcc polycrystals and for other crystal structures.

3. *Strengthening of Metal Matrices by Rigid Particles*

The macroscopic strength of particle-reinforced metal-matrix composites is found to depend upon particle diameter in addition to volume fraction, for particle diameters in the range 0.1 μm to 10 μm. For example, Lloyd (1994) has tested a composite of silicon carbide particles in

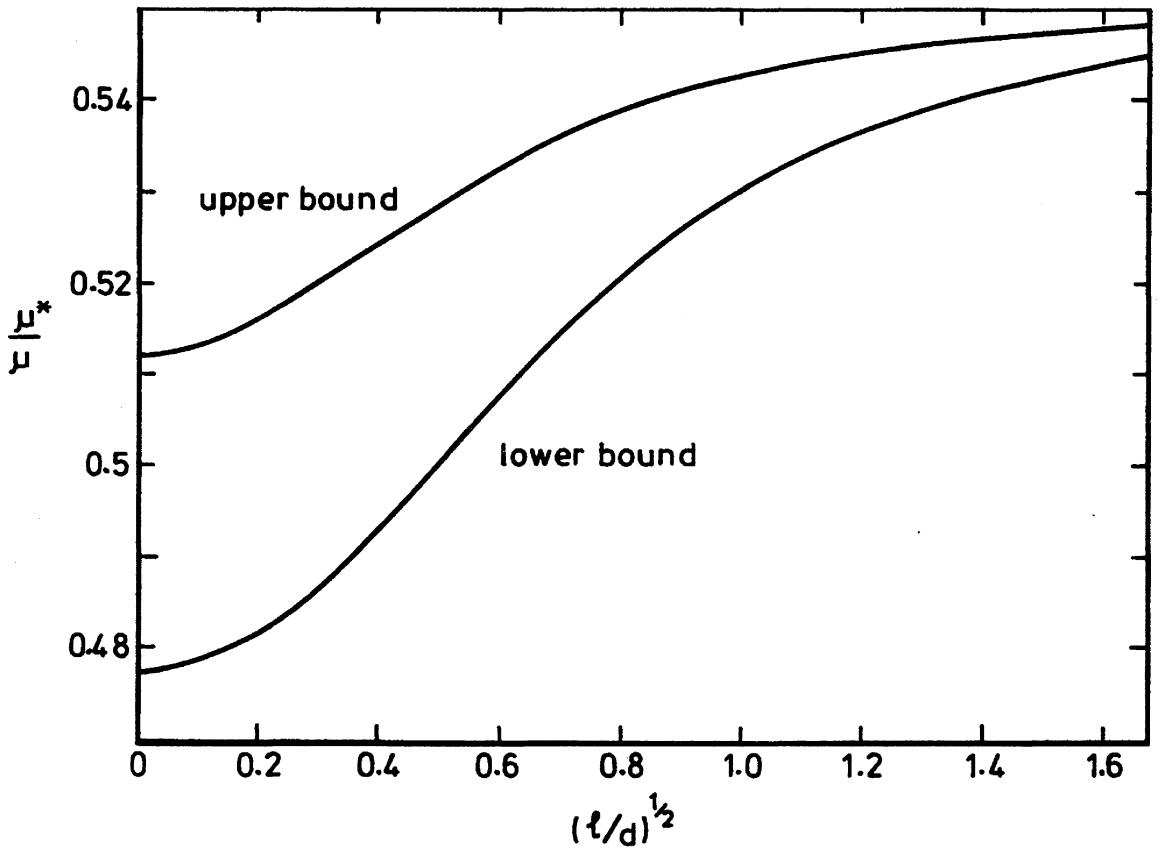

FIG. 5. Hashin-Shtrikman upper and lower bounds on the macroscopic shear modulus μ^* for an isotropic face-centered cubic polycrystal. Each grain of dimension d is assumed to deform by slip on 12 independent slip systems. The slip response is taken as linear elastic with a strain energy density function given by expression (2.32), involving the material length scale ℓ. Taken from Smyshlyaev and Fleck (1996).

an aluminium-silicon matrix. He observed a 10% increase in the strength when the particle diameter was reduced from 16 μm to 7.5 μm with the particle volume fraction fixed at 15%. These particles are sufficiently large that it is thought that plastic deformation is by the interaction of dense clouds of dislocations with each particle rather than by individual dislocation interactions. Nevertheless, conventional continuum plasticity (Bao *et al.*, 1991) predicts that the size of the particles (with the volume fraction fixed) should have no effect on the composite yield strength. As in the previous examples, this follows from the absence of a material-length scale in the conventional theory using simple dimensional considerations. Steep plastic gradients adjacent to each particle necessitate the existence of geometrically necessary dislocations and associated local hardening, as argued by Ashby (1970) and Brown and Stobbs (1976). These gradients provide the rationale for turning to an approach based on strain gradient plasticity when the particles are micron-sized or smaller.

Fleck and Hutchinson (1993) predicted a strong size effect for a dilute volume fraction ρ of isotropically distributed rigid spherical particles of radius a in a matrix of power law strain gradient solid characterized by (2.2) and (2.1). In uniaxial tension, the average macroscopic stress $\bar{\sigma}$ of the composite is related to its average macroscopic strain $\bar{\varepsilon}$ by

$$\bar{\sigma} = \Sigma_0 \left\{ 1 + \rho \left(\frac{n+1}{n} \right) f_p \right\} \left(\frac{\bar{\varepsilon}}{\mathscr{E}_0} \right)^{1/n} \tag{2.33}$$

where the factor $\rho(n+1)f_p/n$ is the relative strengthening due to the particles at a given strain $\bar{\varepsilon}$. Fleck and Hutchinson (1993) calculated the factor f_p for the CS solid in (2.20), and the results are repeated here in Figure 6: f_p is plotted as a function of ℓ/a for selected values of n as solid line curves. It is noted that f_p increases dramatically with increasing ℓ/a. The role played by the strain hardening index n on this factor is more modest, with a small decrease in f_p with increasing n.

Additional calculations have been carried out to investigate the role played by stretch gradients acting in concert with rotation gradients on the strengthening due to a dilute concentration of rigid particles. Eq. (2.33) remains valid, and results for f_p are included in Figure 6 as dashed line curves for the SG solid in (2.20). The contribution of $\ell_1^2 \eta'^{(1)}_{ijk} \eta'^{(1)}_{ijk}$ to the strain energy density w leads to enhanced strengthening at finite ℓ/a. For example, at $\ell/a = 1$ the full-strain gradient theory predicts 50% more strengthening than that predicted for the couple-stress solid, for all values of n considered.

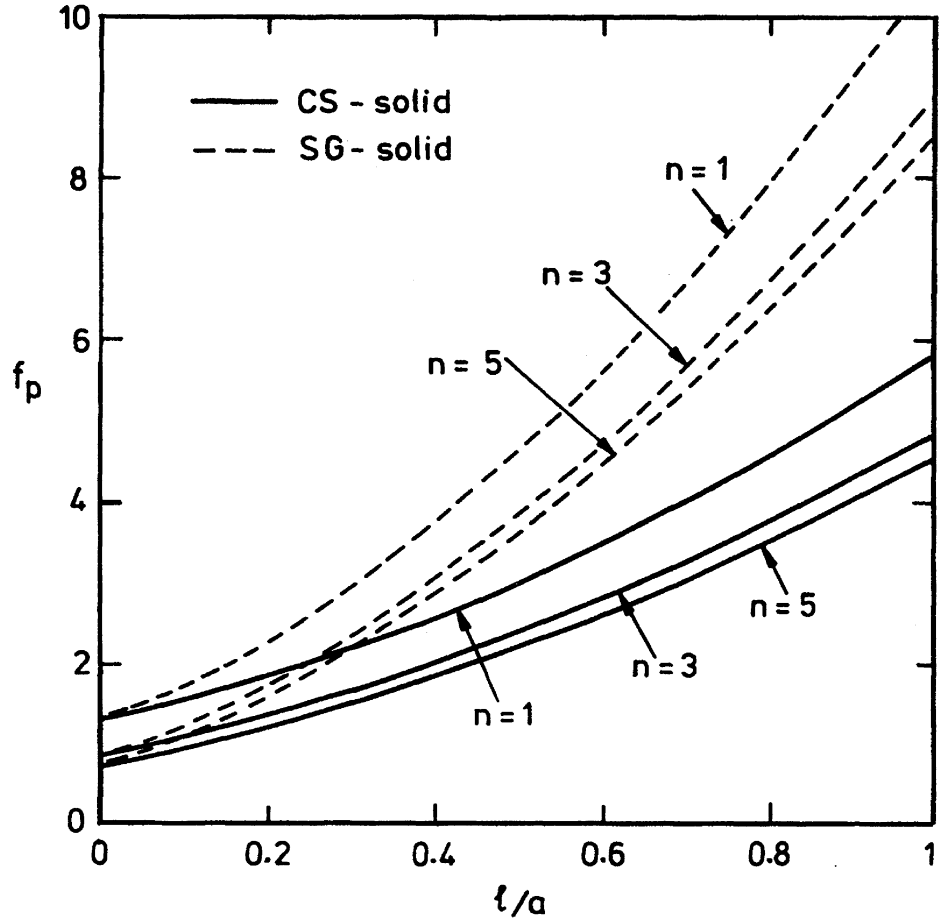

FIG. 6. The effect of particle radius a on the macroscopic strengthening f_p of a strain gradient deformation theory solid. Results are given for both the stretch-gradient (SG) solid and for the couple stress (CS) solid (taken from Fleck and Hutchinson, 1993). In all cases $\mu = 2$.

The influence of the parameter μ in (2.23) on f_p is displayed in Figure 7 for the two solids. Numerical difficulties in the solution process are encountered for values of μ close to 1, and thus the smaller value of μ used in Figure 7 is 1.25. The trend of the prediction for the smaller value of μ can be approximately reproduced using $\mu = 2$ if a large value of ℓ/a is chosen. However, as was the case for wire torsion, one concludes that the form of the interaction between strain hardening and strain gradient hardening as reflected by the parameter μ may be deserving of further attention, particularly because of the differences in behavior at small values of ℓ/a.

There is experimental and theoretical evidence to suggest that the size of each phase in a two-phase alloy has an effect on the macroscopic strength (Funkenbusch and Courtney, 1985; Funkenbusch *et al.*, 1987; Smyshlyaev and Fleck, 1994, 1995). Specifically, it is observed that the

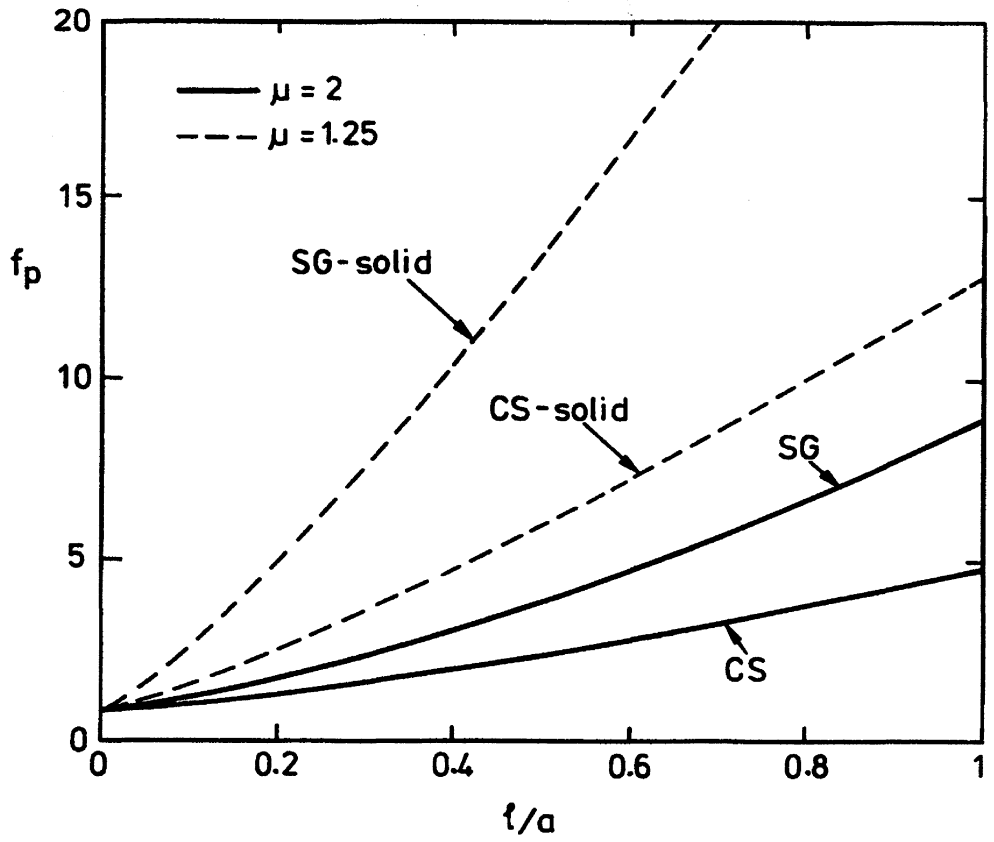

FIG. 7. The influence of the parameter μ in (2.23) on f_p, for particle strengthening, $n = 3$.

smaller the size of each phase, the greater is the strength. The two-phase alloy bridges the two extremes of a metal matrix composite containing rigid particles and a single-phase alloy. Since a size effect is noted at both limits, it is not surprising that a size effect is also observed for the two-phase alloy.

4. *Void Growth and Softening: The Role of Void Size*

A common fracture mechanism of ductile metals is nucleation, growth, and coalescence of voids. There exists a well-defined mechanics of void growth based on conventional continuum plasticity theory (e.g., Rice and Tracey, 1969; Gurson, 1977; Needleman *et al.*, 1992; Tvergaard, 1990). None of the widely used results from the literature on void growth involve any dependence on void size, even though they are sometimes applied to voids of micron or even sub-micron size. There is some indirect evidence that voids in the micron to sub-micron size range are less susceptible to growth at a given stress state than larger voids (private communication from A. G. Evans, 1996), but a careful experimental examination of this issue remains to be carried out. It is of interest to study theoretically the

effect of void size upon void growth and the associated macroscopic softening within the context of the present class of strain gradient theories. We shall see that void growth strongly distinguishes between gradient effects tied solely to rotation gradients versus those arising as well from stretch gradients. Moreover, void growth phenomena may provide a robust means for confronting strain gradient plasticity predictions with experiment.

Consider the problem of an isolated spherical void of radius a in an infinite, incompressible power law matrix which has been addressed in most prior work, but with a matrix characterized by w in (2.21) with the effective strain (2.15). The solid is subjected to uniform remote axisymmetric loading specified by $\sigma_{33}^{\infty} = S$ and $\sigma_{11}^{\infty} = \sigma_{22}^{\infty} = T$ with $S > T$, as depicted in the insert in Figure 8(a). As in previous work, it is convenient to employ the remote mean stress $\sigma_m^{\infty} \equiv \frac{1}{3}S + \frac{2}{3}T$ and the remote deviatoric stress $\sigma^{\infty} \equiv S - T$, and to introduce the non-dimensional measure of stress triaxiality as $X \equiv \sigma_m^{\infty}/\sigma^{\infty}$. The remote strain follows from $\sigma_{ij} = \partial w/\partial \varepsilon_{ij}$ as

$$\varepsilon_{33}^{\infty} = \mathscr{E}_0(\sigma^{\infty}/\Sigma_0)^n, \quad \varepsilon_{11}^{\infty} = \varepsilon_{22}^{\infty} = -\frac{1}{2}\varepsilon_{33}^{\infty} \tag{2.34}$$

Calculations have been performed on the volume expansion increment $\dot{V}$ of an isolated void of volume V in the infinite matrix subjected to an increment of axisymmetric loading specified by $\dot{\varepsilon}_{33}^{\infty}$. Calculations have been performed for each of the two strain-gradient solids given by (2.20). The problem for the CS solid, for which w depends solely on the rotation gradients, was previously analyzed by Fleck and Hutchinson (1993). Results for the normalized dilation rate, $\dot{V}/\dot{\varepsilon}_{33}^{\infty}V$, have the functional form

$$\frac{\dot{V}}{\dot{\varepsilon}_{33}^{\infty}V} = F\left(X, \frac{\ell}{a}, n\right) \tag{2.35}$$

It is through the dependence on ℓ/a that void size produces behavior different from that for the conventional power law solid.

Representative results are given in Figure 8(a) for the normalized dilation rate as a function of ℓ/a for the stress triaxiality in uniaxial tension, $X = 1/3$, and the triaxiality representative of that directly ahead of a mode I crack tip in plane strain, $X = 2.5$. This figure illustrates the sharp differences in the void growth behavior implied by the two constitutive models, CS and SG, which were alluded to above. The limit for $\ell/a = 0$ is the result for the conventional solid. There is very little effect of

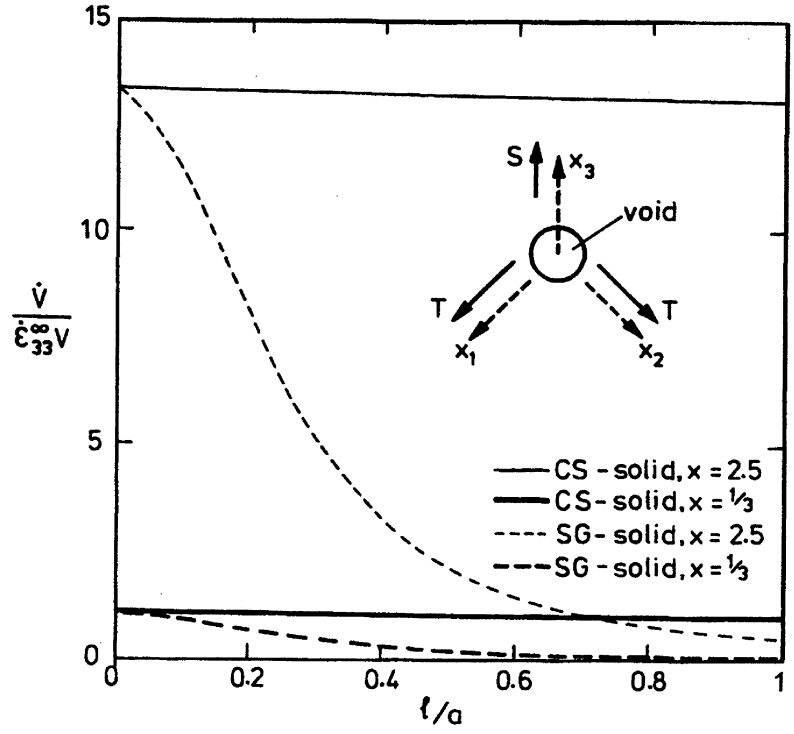

(a)

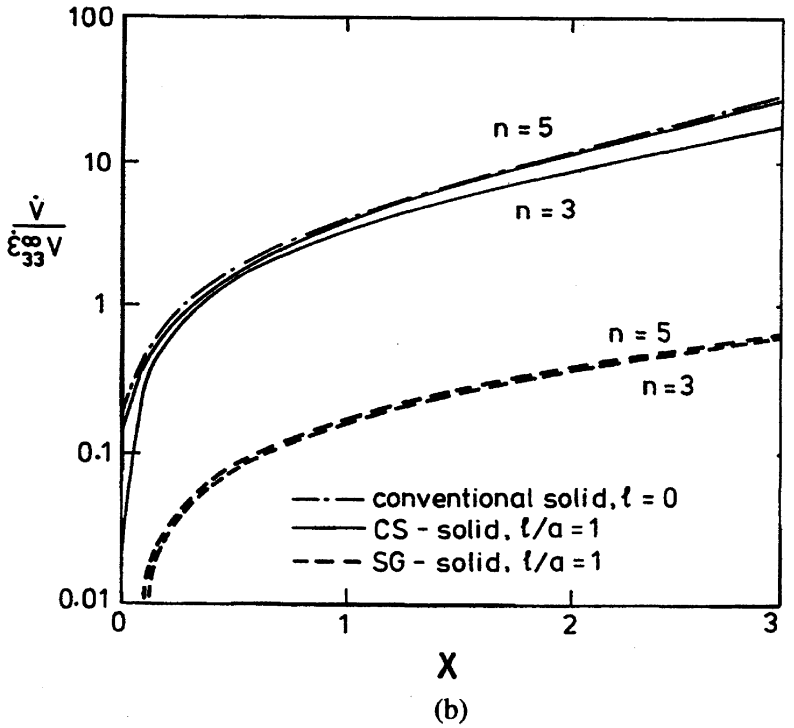

(b)

FIG. 8. Growth rate of an isolated void under remote axisymmetric loading: axial stress S and transverse stress T. The stress triaxiality X is defined by $X \equiv (S + 2T)/3(S - T)$. a) Effect of void radius a upon normalized void growth rate, for $n = 3$. b) Effect of stress triaxiality X upon normalized void growth rate.

void size upon the normalized dilation rate for the CS solid at both triaxialities. This is readily understood when it is recognized that the dominant deformation field in the vicinity of void producing its expansion is the spherically symmetric radial displacement field. The radial displacement field is irrotational inducing no rotation gradients and, therefore, no strain gradient contribution to the strain energy density w for the CS solid.

By contrast, the spherically symmetric radial field does induce significant gradients of stretch, leading to the exceptionally strong reduction of growth rates for smaller voids in the SG solid relative to larger voids seen in Figure 8(a). In effect, the expanding void is surrounded by a shell of hardened material due to the presence of both strain and strain gradient hardening. The authors are unaware of any existing experiments against which to test these predictions. Typically, metals contain a distribution in size of pre-existing void-nucleating defects such as soft inclusions and particles with weak interfaces. When stretch gradients influence hardening, strain gradient theory suggests that only voids larger than some cut-off size will grow and coalesce; smaller voids should experience little growth. Several other phenomena will be discussed later in this survey which display a similarly strong selectivity to stretch gradients over rotation gradients due to the character of their deformation fields. One is the closely related phenomenon of cavitation instability, and another is the indentation hardness test. It seems reasonable to hope that careful experimental observations related to these phenomena, in conjunction with tests where rotation gradients are dominant, should provide a means to identify which of the competing constitutive models best reproduce small scale behavior.

For completeness, void growth is plotted in Figure 8(b) as a function of triaxiality ratio for three solids: the conventional solid (i.e., $\ell/a = 0$), the CS solid with $\ell/a = 1$, and the SG solid with $\ell/a = 1$. Results are presented for both $n = 3$ and $n = 5$. It is clear from the figure that the couple-stress solid displays almost the same rate of void growth as the conventional solid at all stress triaxialities. In contrast, for all triaxilities, the rate of void growth is reduced by about an order of magnitude for the SG solid compared with the conventional solid.

There is a close connection between the reduction in void growth due to strain gradient effects and the reduction in macroscopic softening due to the presence of the voids, as the counterpart to particle strengthening. The same power law metal matrix discussed above is considered which contains an isotropically distributed dilute population of spherical voids of radius a.

The porous solid is subject to the overall, or macroscopic, axisymmetric stress state characterized by S and T with triaxiality X as defined above. With $\bar{\sigma}_{ij}$ and $\bar{\varepsilon}_{ij}$ as the macroscopic stresses and strains and $\Phi(\bar{\sigma}_{ij})$ as the strain potential such that $\bar{\varepsilon}_{ij} = \partial\Phi/\partial\sigma_{ij}$, Fleck and Hutchinson (1993) have shown that a dilute concentration ρ of voids alters Φ to

$$\Phi = \Sigma_0 \mathscr{E}_0 \left(\frac{\bar{\sigma}_c}{\Sigma_0}\right)^{n+1} \left\{\frac{1}{n+1} + \rho f_v\left(X, \frac{\ell}{a}, n\right)\right\} \tag{2.36}$$

The function f_v can be computed from the solution for the isolated spherical void in the infinite matrix (F in (2.35) is related to f_v by $F = \partial f_v/dX$). The larger is f_v, the larger is the strain at a given stress, or, equivalently, the greater is the softening at a given strain. Plots of f_v versus the triaxiality factor are given in Figure 9 for the same three solids considered in the previous figure: the conventional solid ($\ell/a = 0$) and the CS and SG solids, each with $\ell/a = 1$. Again it is seen that there is little difference between the softening predicted for the conventional solid and the CS solid, with both predicting a large increase in softening as triaxiality increases. When stretch gradients are assumed to contribute to

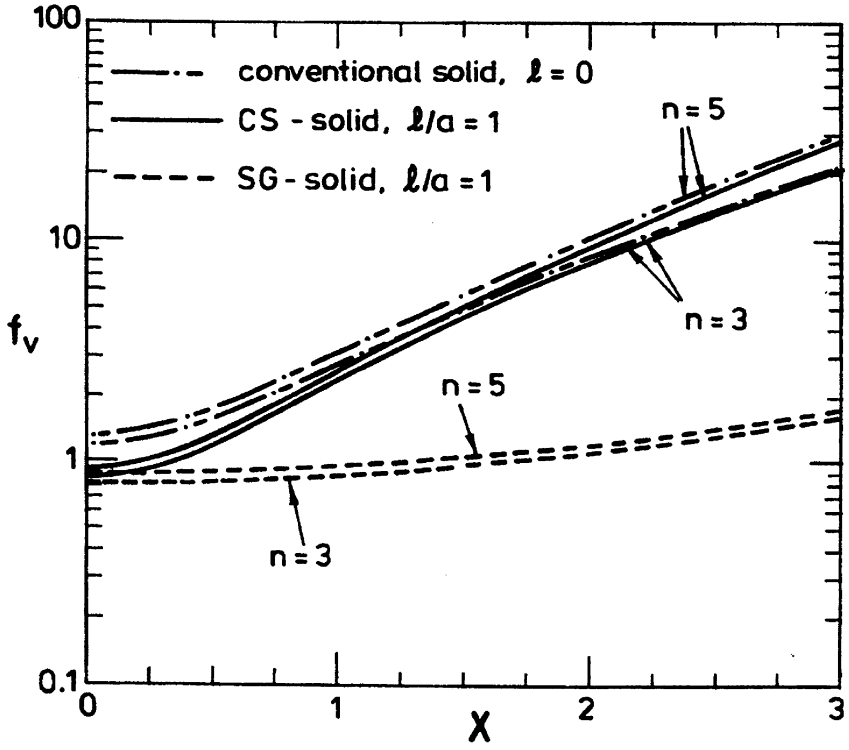

FIG. 9. The effect of stress triaxiality X upon the macroscopic softening f_v for an isolated void.

hardening, as in the case of the SG solid, softening is significantly moderated, especially at large triaxiality.

In other work, Gologanu *et al.* (1995) have taken the first steps to address a strain gradient theory for porous metals by generalizing the Gurson (1977) model to include the effect of macroscopic strain gradients. They do not address the issue of local strain gradients on the growth of the voids, as done here. Instead, these authors retain the assumption that the material surrounding the voids is a classical elastic-plastic solid. They derive a modified yield function for applications where the gradient of strains is such that the deformation scale begins to become comparable to the void spacing. Their results are somewhat surprising in that the dominant effect of the strain gradient is not influenced by the void volume fraction or void spacing, and, moreover, the gradient effect persists as the volume fraction approaches zero.

5. *Cavitation Instabilities*

A void in an elastic-plastic solid will grow unstably at sufficiently high mean stresses in what is usually described as a cavitation instability (Bishop *et al.*, 1945). Strain gradients will delay cavitation to larger mean stresses when the void size is comparable to ℓ, assuming the solid experiences hardening due to stretch gradients. In this section, results from M. Begley (work in progress) will be presented for the effect of strain gradients on the cavitation instability of a spherical void of initial radius a in an infinite, incompressible solid subject to a spherically symmetric radial loading at infinity. In the notation used above, the remote stress is specified by $S = T$ so that the remote mean stress is $\sigma_m^\infty = S$. An isotropic solid containing a spherical void undergoes spherically symmetric deformations such that there are no rotations and, therefore, no rotation gradients. Thus, of the two solids in (2.20), only the SG solid will produce a strain gradient effect through its dependence on stretch gradients. The only strain gradient term to survive in (2.19) is the term with coefficient ℓ_1^2, and $\mathscr{E}$ reduces to

$$\mathscr{E}^2 = \frac{2}{3}\varepsilon'_{ij}\varepsilon'_{ij} + \frac{5}{2}\ell^2\left(\frac{\partial \varepsilon_{rr}}{\partial r}\right)^2 = \varepsilon_e^2 + \frac{5}{2}\ell^2\left(\frac{\partial \varepsilon_e}{\partial r}\right)^2 \qquad (2.37)$$

where r denotes the radial coordinate and, as before, $\ell \equiv \ell_1$. Cavitation is driven by the elastic energy stored in the remote field, and therefore it is essential to include linear elastic strains in the constitutive model. To this

end, the power law SG solid, (2.21) with (2.37), is coupled to an incompressible linear elastic range according to

$$\begin{aligned} w &= \frac{1}{2}E\mathscr{E}^2 && \text{for } \mathscr{E} < \mathscr{E}_0 \\ &= \Sigma_0\mathscr{E}_0\left\{\frac{n}{n+1}\left[\left(\frac{\mathscr{E}}{\mathscr{E}_0}\right)^{(n+1)/n} - 1\right] + \frac{1}{2}\right\} && \text{for } \mathscr{E} \geq \mathscr{E}_0 \end{aligned} \tag{2.38}$$

where E is Young's modulus and the connection $\Sigma_0 = E\mathscr{E}_0$ is required. In uniaxial tension, this gives $\varepsilon = \sigma/E$ for $\sigma < \Sigma_0$ and $\varepsilon = \mathscr{E}_0(\sigma/\Sigma_0)^n$ for $\sigma > \Sigma_0$. Here, Σ_0 is to be regarded as the initial tensile yield stress and $\mathscr{E}_0$ as the associated tensile yield strain. The inclusion of a strain gradient dependence in the linear elastic range through $\mathscr{E}$ is only for mathematical convenience. It has essentially no influence on the cavitation stress since the strain gradients in the elastic region are very small.

The cavitation analysis for the strain gradient solid parallels that given for the conventional elastic-plastic solid given by Huang *et al.* (1991). The results presented below are obtained using an exact finite strain analysis in which ε_e is the logarithmic strain and r is the radial coordinate in the deformed state. However, Begley established that finite strain effects do not have a major influence on the solution. The cavitation stress, σ_c, is the remote mean stress at which the void grows without bounds, i.e., $dV/d\sigma_m^\infty \to \infty$. It has the following dimensionless form

$$\sigma_c/\Sigma_0 = F(N, \Sigma_0/E, \ell/a) \tag{2.39}$$

where $N = 1/n$. Values of σ_c/Σ_0 for the conventional solid ($\ell/a \to 0$) are presented by Huang *et al.* (1991); $[\sigma_c]_{\ell=0}/\Sigma_0$ lies between 4 and 8 for values of N and Σ_0/E typical of metals. Here we display plots of the normalized cavitation stress as the ratio $\sigma_c/[\sigma_c]_{\ell=0}$, thereby emphasizing the effect of the strain gradients. The normalized cavitation stress is shown as a function of ℓ/a for various N with $\mathscr{E}_0 = 0.003$ in Figure 10(a), and for various $\mathscr{E}_0$ with $N = 0$ in Figure 10(b). The effect is a strong one according to the assumed material model. Voids with radii less than about 2ℓ will have a significantly enhanced resistance to cavitation relative to larger voids.

6. *Indentation Hardness Testing*

Size effects have been recognized in indentation hardness testing for some time. Various factors can give rise to a hardness measurement which depends on the size of the indentation, including surface effects and the

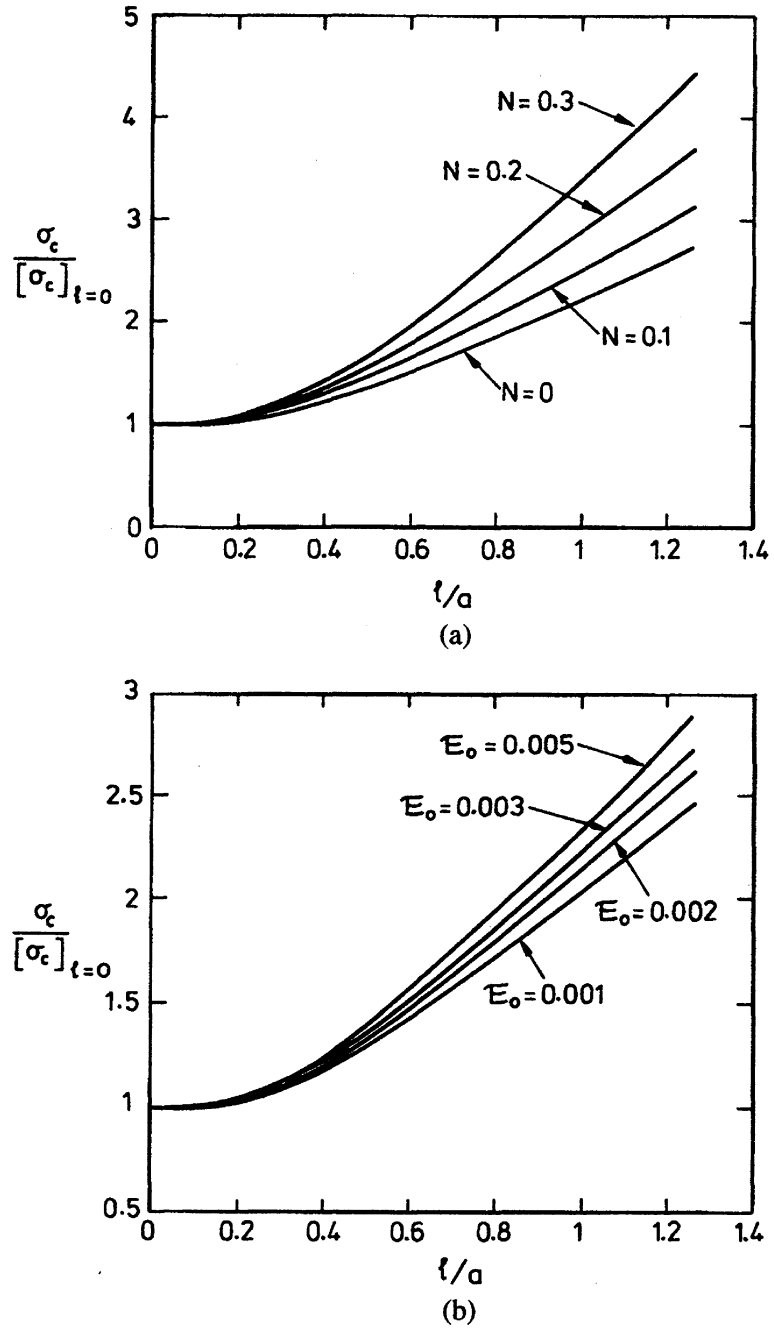

FIG. 10. a) The normalized cavitation stress $\sigma_c/[\sigma_c]_{\ell=0}$ as a function of ℓ/a. a) effect of strain hardening exponent N, with $\mathscr{E}_0 = 0.003$, b) effect of yield strain $\mathscr{E}_0$, with $N = 0$.

absence of nearby dislocation sources for nano-scale indents. However, as mentioned in the Introduction in connection with the hardness data in Figure 1, there appears to be clear evidence of a strong indentation size dependence in the range of micron to sub-micron indents which is due to the increasing dominance of geometrically necessary dislocations as indents become smaller (Poole *et al.*, 1996; Stelmashenko *et al.*, 1993; Ma

and Clarke, 1995; Nix, 1988). The scale is sufficiently large for very large numbers of dislocations to be involved: consequently, this is another example where a continuum plasticity approach would appear to be required for quantitative analysis. The simplicity of the indentation test and the availability of equipment for conducting micro-indentations suggests that this test may be a good candidate for measuring the material length scale, ℓ, in the strain-gradient constitutive model.

Work is underway to analyze the test for several indenter head shapes, applied to both polycrystalline and single-crystal materials. At this writing, the only results available are those by Shu and Fleck (1996) for axisymmetric frictionless indenters applied to the CS material. Three head shapes were considered: flat-ended, conical, and spherical and only a minor effect of head shape was found for indentation of the non-linear solid. In addition, results were obtained for a flat-ended circular punch with sticking friction. Shu and Fleck (1996) obtained their indentation results by the finite element method, with elements designed to capture the strain-gradient dependence. The calculations have been performed without accounting for finite strain effects, but earlier studies on indentation of conventional elastic-plastic solids indicated that finite strain effects should not alter the hardness predictions by more than a few percent (Bower *et al.*, 1993).

The results of Shu and Fleck (1996) are repeated here for the flat-headed indenter of radius a. The indenter is pushed into a semi-infinite half-space of the elastic-plastic CS material specified by (2.38) and (2.20). Two conditions at the interface between the indenter and the half-space have been considered: frictionless contact and fully sticking contact with no sliding. The load P applied to the indenter approaches an asymptote $P_{\max}$ as the indenter is forced down into the half-space. The hardness is defined to be $H = P_{\max}/(\pi a^2)$. For the problem posed it has the form

$$H = \Sigma_0 F(n, \ell/a, \varepsilon_0) \tag{2.40}$$

where the dimensionless function F depends on which of the two contact conditions are operative. The dependence on the initial yield strain ε_0 is weak; the results presented in Figure 11 have been computed with $\varepsilon_0 = 0.01$. The results in this figure bring out the role of strain gradients by normalizing H at a given ℓ/a by the corresponding hardness prediction for the conventional solid (with $\ell = 0$). There is an appreciable dependence on the assumed contact condition. The size dependence for the frictionless indenter is rather small, while that for the indenter with no sliding is somewhat more substantial. Indentation is not unlike void growth

or cavitation in that the indenter forces a 'radial' outward expansion of the material. The contribution to the deformation field from this outward expansion produces relatively small rotations. Thus, as in the case of the other two phenomena, indentation is not expected to give rise to a very large strain gradient effect for the CS solid. The sticking indenter induces more shearing and rotation than the frictionless indenter, and this is the qualitative explanation for the difference between the two cases.

It would appear that the indentation hardness test is another instance for which a hardness dependence on stretch gradients will greatly influence the predicted size effect. Work is currently underway to calculate these effects for indenters, conical and flat-headed, forced into the SG solid. The expectation is that the size effects for this solid will be considerably larger than those evident in Figure 11.

7. *The Stress Field in the Vicinity of a Sharp Crack Tip*

Attempts to link macroscopic fracture behavior to atomistic fracture processes in ductile metals are frustrated by the inability of conventional plasticity theories to adequately model stress-strain behavior at the small scales required in crack-tip models. This does not appear to be an issue for metals whose fracture process is void growth and coalescence since the process zone is usually measured in tens or even hundreds of microns. It is

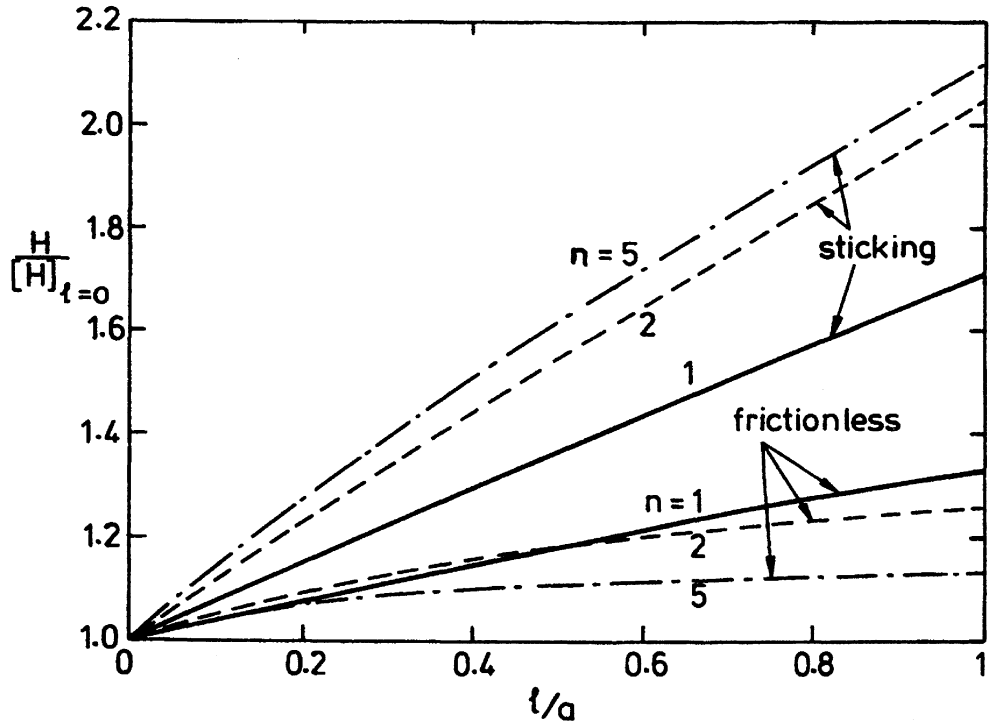

FIG. 11. The normalized indentation hardness $H/[H]_{\ell=0}$ for a flat-ended circular punch. Results are presented for both the frictionless and sticking cases, for a range of values of strain hardening exponent n.

a major issue when the fracture process is atomic separation. Conventional plasticity theory is unable to explain how stresses at a sharp crack tip can reach levels necessary to bring about atomic decohesion at the tip of a sharp crack where the relevant scale is far below the micron level. The high-strain gradients invariably present near the crack tip in an elastic-plastic solid suggest that there should be an annular zone surrounding the tip within which geometrically necessary dislocations play a role in elevating the local hardening and, therefore, the stress levels near the tip. A discussion of a number of the open issues surrounding the goal of bridging from the macroscopic level where loads are applied to the crack tip where the fracture process occurs is given in the article by Bagchi and Evans (1996).

Some progress has been made in applying strain-gradient plasticity theory to the estimation of crack tip fields by Huang *et al.* (1995), Xia and Hutchinson (1996), and Schiermeier and Hutchinson (1996). Thus far, only the CS solid has been considered in these studies. We begin the discussion in this section by first considering the more general elastic-plastic deformation theory SG solid depending on both rotation and stretch gradients, such as the power-law solid in (2.21) where the generalized strain quantity $\mathscr{E}$ is defined by (2.19).

For plane strain and mode III crack problems, a J-integral exists for this material which equals the energy release rate of the crack when evaluated on a contour circling the crack tip in the usual manner. Application of the J-integral to the crack-tip problem implies that the energy density w must have a r^{-1} singularity, where r is the distance from the tip. This same conclusion is reached for the conventional solid, leading directly to the general form of the HRR crack tip fields for a power-law material. The form of the singular fields is different for the general strain gradient solid. For the general solid, the strain gradients $\boldsymbol{\eta}$ will dominate the strains $\boldsymbol{\varepsilon}$ as the crack tip is approached. Since $\mathscr{E}$ must have a $r^{-n/(n+1)}$ singularity for $w \to r^{-1}$, it follows that $\boldsymbol{\eta}$ must also have a $r^{-n/(n+1)}$ singularity. The dominant quantities in the crack tip singularity field can be written in a form analogous to that for the HRR fields for the conventional power-law solid:

$$\eta_{ijk} = \ell^{-1}\mathscr{E}_0\left(\frac{J}{\Sigma_0\mathscr{E}_0 C_n r}\right)^{n/(n+1)} \tilde{\eta}_{ijk}(\theta, n),$$

$$\tau_{ijk} = \ell\Sigma_0\left(\frac{J}{\Sigma_0\mathscr{E}_0 C_n r}\right)^{1/(n+1)} \tilde{\tau}_{ijk}(\theta, n) \tag{2.41}$$

where C_n is a normalizing constant and (r, θ) are planar polar coordinates centered at the tip. The θ-variations, $\tilde{\eta}_{ijk}$ and $\tilde{\tau}_{ijk}$, depend on the choice of normalization and on which of the modes, I, II or III, pertains. They also depend on the particular combination of the material length parameters, ℓ_1, invoked for the material model (e.g., as in (2.20)). In the general case, the stress and strains are less singular than the quantities in (2.41). More importantly, however, is the fact that the higher order stresses τ_{ijk} contribute to the tractions in proportion to their gradient—see ahead to eq. (3.8) in Section III. Thus, tractions $\mathbf{t}$ acting on material surfaces will be strongly singular according to $\mathbf{t} \to r^{-(n+2)/(n+1)}$. It follows that the tractions near the tip of a sharp crack in the general strain gradient solid will be significantly higher than the tractions near the crack tip in the conventional solid.

The mode III crack The analytical features outlined above have been detailed for the mode III crack (Schiermeier and Hutchinson, 1996). For the antiplane shearing deformations of mode III no stretch gradients occur. Thus, the general solid reduces to a solid which depends only on rotation gradients in anti-plane shear, and, as a consequence, the problem fits within the framework of couple stress theory. The mode III crack study investigated the influence of the two rotation-gradient invariants in (2.19), $\chi'_{ij}\chi'_{ij}$ and $\chi'_{ij}\chi'_{ji}$, with the finding that the $\chi'_{ij}\chi'_{ji}$ invariant plays a secondary role. Thus, with little loss in generality, the mode III crack in the general solid can be replaced by the problem for the crack in the CS solid, similar to the exact reduction which applies for wire torsion. The full details of the singular crack-tip fields in (2.41) have been worked out for the mode III problem. Numerical results have been obtained using a finite element scheme for the full field, merging the singular fields with the outer HRR field whose amplitude is specified as J. (For the pure power material, the HRR field is a solution to the field equations at large r.) The transition from the outer HRR solution to the inner singular field (2.41) occurs smoothly over the annular region centered at the tip roughly equal to $\frac{1}{2}\ell < r < 5\ell$. This transition is illustrated by the behavior of the shearing displacement of one face of the crack relative to the other, δ, displayed in Figure 12. The normalization of δ on the ordinate is a consequence of the choice r/ℓ as the abscissa. The three curves shown are the HRR solution, the asymptotic solution from the singular field (2.41), and the full finite-element solution to the problem. The r-dependence of δ associated with (2.41) is $\delta \to r^{(n+2)/(n+1)}$, and it can be seen that the full numerical-

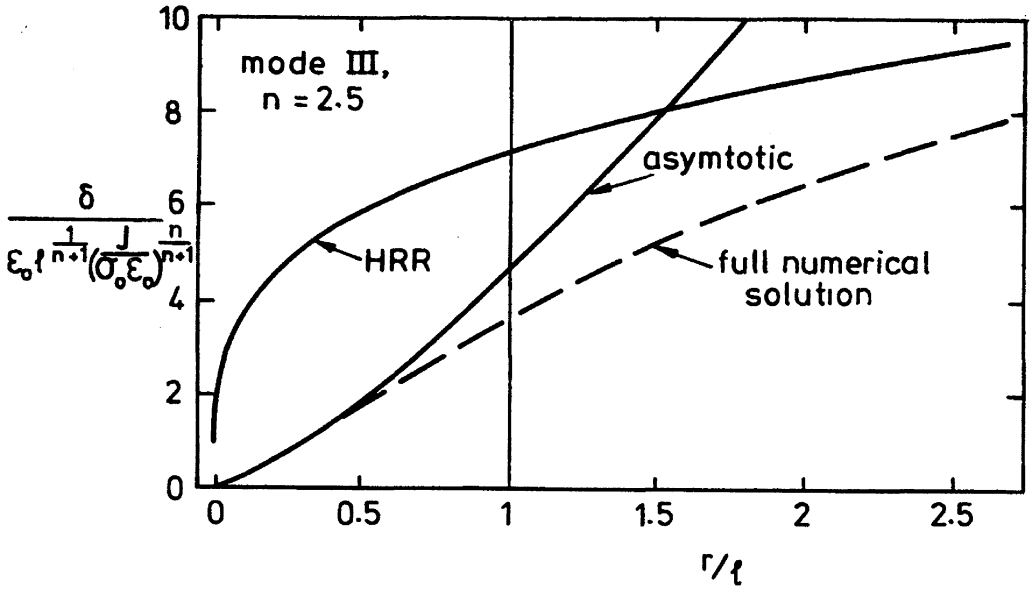

FIG. 12. The shear displacement profile near the tip of a mode III crack in the CS-solid.

solution asymptotes to the near-tip solution. The full solution also asymptotes to the HRR solution once r/ℓ exceeds about 5.

Mode I and II crack solutions Although no results have yet been obtained for mode I or II cracks in the *general* strain gradient (SG) solid, it is expected that many of the qualitative features of the solution described for the mode III crack will apply to the plane strain-crack problems as well. We note in passing that for the general case of plane-strain deformation, such as the mode I or II crack-tip fields, the combined strain quantity, $\mathscr{E}$, and hence the strain density, w, can be written solely in terms of the invariants $\varepsilon'_{ij}\varepsilon'_{ij}$, $\eta'^{(1)}_{ijk}\eta'^{(1)}_{ijk}$ and $\chi'_{ij}\chi'_{ij}$ since the invariant $\chi'_{ij}\chi'_{ji}$ vanishes identically. Thus, the most general material in this class is represented by (2.19) with only two length parameters, ℓ_1 and a second parameter proportional to $(4\ell_2^2/3 + 8\ell_3^2/5)^{1/2}$. Quite another result from that described above has been obtained for plane-strain cracks in the CS solid, whose strain-gradient contribution to hardening, one should recall, depends only on the rotation gradients. Unexpectedly, it turns out that the singular field for the plane-strain problems is irrotational (Huang *et al.*, 1991; Xia and Hutchinson, 1996). Consequently, rotation gradients vanish in the dominant singular field, as does the invariant $\chi'_{ij}\chi'_{ij}$. The argument leading to (2.41) no longer applies for the plane-strain crack in the CS solid, since the strain-gradient contribution to $\mathscr{E}$ does not dominate the contribution from ε_e as $r \to 0$. (This possibility is excluded in the mode III problem because no irrotational singular field exists.) The outcome of the full analysis of the plane-strain crack problems for the CS solid is that ε_e is dominant in the singular field and the requirement that $w \to r^{-1}$ leads

to a singular field with $\boldsymbol{\varepsilon} \to r^{-n/(n+1)}$ and $\boldsymbol{\sigma} \to r^{-1/(n+1)}$. This is the same r-dependence for the stresses and strains in the HRR field. Nevertheless, the two fields are not the same. The HRR field is *not* irrotational; moreover, the gradients of $\boldsymbol{\tau}$ in the CS crack problem are of the same order as $\boldsymbol{\sigma}$, and therefore make their presence felt in the singular field.

As in the case of the mode III problem, the plane-strain HRR solution satisfies the field equations for the power law CS solid as $r \to \infty$. Given the observations above, the general form of the solution to the full problem for a semi-infinite plane-strain crack in the CS solid with the HRR field imposed as $r \to \infty$ can be written as follows (Xia and Hutchinson, 1996):

$$\begin{aligned}
\left[\varepsilon_{ij}, \ell\chi_{ij}\right] &= \mathscr{E}_0\left(\frac{J}{\Sigma_0\mathscr{E}_0 I_n r}\right)^{n/(n+1)}\left[\tilde{\varepsilon}_{ij}\left(\theta, \frac{r}{\ell}, n\right), \tilde{\chi}_{ij}\left(\theta, \frac{r}{\ell}, n\right)\right] \\
\left[\sigma_{ij}, \ell^{-1}m_{ij}\right] &= \Sigma_0\left(\frac{J}{\Sigma_0\mathscr{E}_0 I_n r}\right)^{1/(n+1)}\left[\tilde{\sigma}_{ij}\left(\theta, \frac{r}{\ell}, n\right), \tilde{m}_{ij}\left(\theta, \frac{r}{\ell}, n\right)\right]
\end{aligned} \tag{2.42}$$

Here, $\mathbf{m}$ is the couple stress tensor whose components represent a subset of the components of $\boldsymbol{\tau}$ as specified in Section III. The quantities $\tilde{\varepsilon}_{ij}$ and $\tilde{\sigma}_{ij}$ approach the corresponding HRR quantities as $r/\ell \to \infty$ (if the normalizing factor I_n is the same as that for the HRR fields) and approach those associated with the singular field as $r/\ell \to 0$. The quantities $\tilde{\chi}_{ij}$ and $\tilde{m}_{ij}$ vanish for both $r/\ell \to 0$ and ∞, but are non zero in the intermediate region connecting the remote field to the crack-tip singular field. Plots of $\tilde{\sigma}_{\pi}$ and $\tilde{\sigma}_{\theta\theta}$ are given in Figure 13 for the mode I crack with $n = 5$. The transition from the HRR solution to the dominate singularity again occurs smoothly over the range from $r/\ell = 5$ to about $1/5$. Surprisingly, the normal stress acting in the plane ahead of the crack tip, $\sigma_{\theta\theta}(\theta = 0)$ is hardly affected by the strain gradient effects in the CS solid. It is anticipated that this is one aspect that will change for a solid whose hardening depends on stretch gradients.

A better understanding of stress elevation required to produce decohesion will require the investigation of the stress fields for the mode I crack for materials whose hardening depends on both the stretch gradients and rotation gradients. As discussed above, the nature of the crack-tip singularity will change to the form given in (2.41) when stretch gradients are included. It seems likely that the more general theory will result in a significant elevation of tractions ahead of a sharp crack, but that remains an open question.

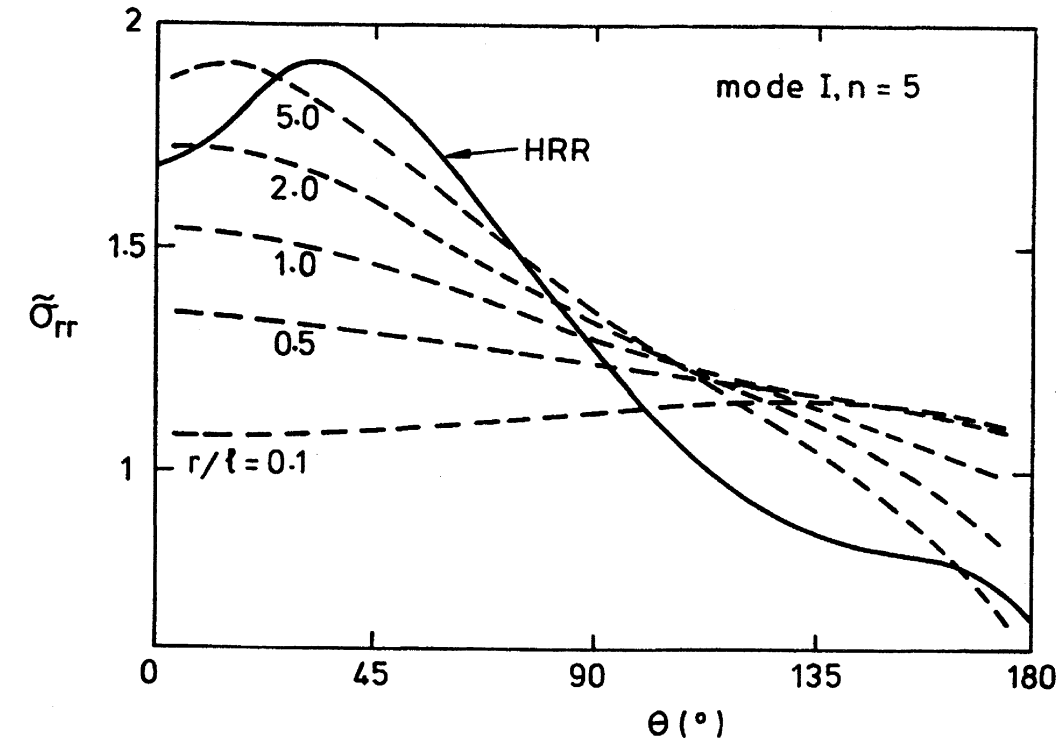

(a)

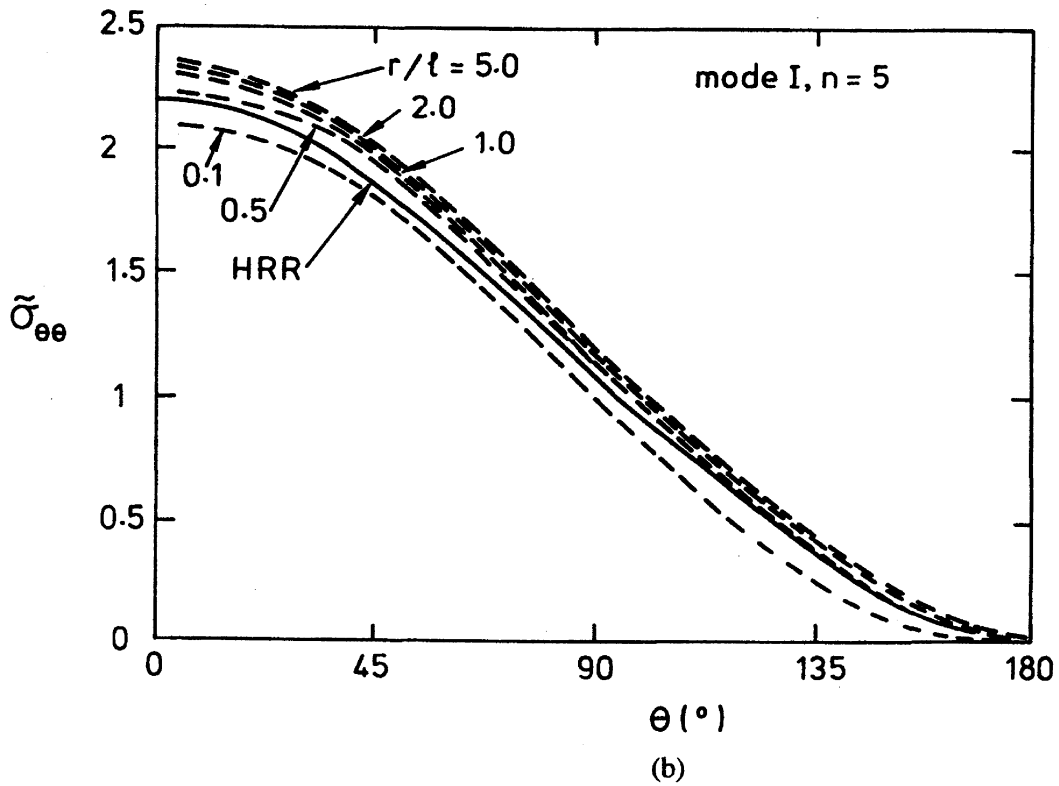

(b)

FIG. 13. Non-dimensional stress field around the tip of a mode I crack for the CS solid, at selected values of radius r from the tip. The non-dimensional stresses are defined in (2.41).

8. *Implications for Further Development of the Theory*

Among the examples discussed above are several for which stretch gradients are absent, such as wire torsion and the Mode III crack, and several for which rotation gradients are either absent or relatively unimportant, such as cavitation, void growth and, possibly, indentation. In the other examples, both types of gradients are present and have the potential for contributing to size effects due to strain gradient hardening. The two sets of examples which are dominated by one type of gradient over the other may provide the best means for the experimental determination of the material-length parameters governing the two types of hardening in the theory.

As has been emphasized in this survey, the objective for developing a strain gradient theory of plasticity is the extension of continuum plasticity to the micron and, possibly, sub-micron range for application to phenomena involving large numbers of dislocations. There is ample evidence that conventional plasticity theories fail to capture the strong size effects which become important at these small scales. Plasticity effects are important in many applications of thin films and multilayers. The thickness of films and layers in some of the applications fall within the scale for which the present theories are intended. Shear lag in thin metal films and layers at edges and corners where they attach to substrates gives rise to significant shear and rotation gradients. Recent experiments on thin film/substrate systems which are cycled thermally to produce plastic deformation display a large film-thickness dependence on yielding and continued plastic flow (private communication from A. G. Evans, 1996). Such effects are well known for very thin epitaxial films where dislocation nucleation is the controlling factor. However, in these experiments the films are polycrystalline and contain large numbers of dislocations, making them candidates for the present class of theories.

III. The Framework for Strain Gradient Theory

A. Toupin-Mindlin Theory

Toupin (1962) and Mindlin (1964, 1965) have developed a theory of linear elasticity whereby the strain energy density w per unit volume depends upon both the symmetric strain tensor $\varepsilon_{ij} \equiv \frac{1}{2}(u_{i,j} + u_{j,i})$ and

the second gradient of displacement $\eta_{ijk} \equiv \bar{\partial}_i \bar{\partial}_j u_k = u_{k,ij}$, where $\bar{\partial}_i$ is the forward gradient operator. Their theory furnishes stress quantities which are work conjugate to the generalized strain variables $\boldsymbol{\varepsilon}$ and $\boldsymbol{\eta}$, and also provides a principle of virtual work. The work increment per unit volume of solid due to an arbitrary variation of displacement $\mathbf{u}$ is given by (2.4) where the symmetric Cauchy stress σ_{ij} is the work conjugate to the strain variation $\delta\varepsilon_{ij}$ and the higher order stress measure τ_{ijk} $(= \tau_{jik})$ is the work conjugate to the strain gradient variation $\delta\eta_{ijk}$. For the special case of a deformation theory solid we may write $w = w(\varepsilon_{ij}, \eta_{ijk})$, giving $\sigma_{ij} = \partial w/\partial \varepsilon_{ij}$ and $\tau_{ijk} = \partial w/\partial \eta_{ijk}$.

Following the strategy of Toupin and Mindlin, the work increment for a volume, V, written

$$\int_V [\delta w]\, dV = \int_V [\sigma_{ij}\, \delta\varepsilon_{ij} + \tau_{ijk}\, \delta\eta_{ijk}]\, dV \tag{3.1}$$

or, via the divergence theorem, as

$$\begin{aligned} \int_V [\sigma_{ij}\, \delta\varepsilon_{ij} + \tau_{ijk}\, \delta\eta_{ijk}]\, dV = &- \int_V \left[\bar{\partial}_i\left(\sigma_{ik} - \bar{\partial}_j \tau_{ijk}\right)\right] \delta u_k\, dV \\ &+ \int_S \left[n_i\left(\sigma_{ik} - \bar{\partial}_j \tau_{ijk}\right)\right] \delta u_k\, dS \\ &+ \int_S \left[n_i \tau_{ijk}\left(\bar{\partial}_j\, \delta u_k\right)\right] dS \end{aligned} \tag{3.2}$$

where n_i is the unit normal to the surface S of the body. The term $\bar{\partial}_j\, \delta u_k$ appears in the last integral on the right-hand side of (3.2). We note that $\bar{\partial}_j\, \delta u_k$ is not independent of δu_k on the surface S because, if δu_k is known on S, so is the surface-gradient of δu_k. In order to correctly identify the independent-boundary conditions in a variational principle we resolve the gradient $\bar{\partial}_j\, \delta u_k$ into a surface-gradient, $D_j\, \delta u_k$, and a normal gradient, $n_j D\, \delta u_k$,

$$\bar{\partial}_j\, \delta u_k = D_j\, \delta u_k + n_j D\, \delta u_k \tag{3.3}$$

where the surface-gradient operator D_j is

$$D_j \equiv (\delta_{jk} - n_j n_k)\bar{\partial}_k \tag{3.4}$$

and the normal gradient operator D is

$$D \equiv n_k \bar{\partial}_k \tag{3.5}$$

To proceed, we substitute (3.3–3.5) into (3.2) and make use of Stokes's surface divergence theory (see for example, Mindlin, 1965) to get the final form for the *principle of virtual work*

$$\int_V [\sigma_{ij}\, \delta\varepsilon_{ij} + \tau_{ijk}\, \delta\eta_{ijk}]\, dV$$

$$= \int_V [f_k\, \delta u_k]\, dV + \int_S [t_k\, \delta u_k]\, dS + \int_S [r_k (D\, \delta u_k)]\, dS \tag{3.6}$$

where the *body force* per unit volume is f_k. The *equilibrium relation* in V is

$$f_k + \bar{\partial}_i \left(\sigma_{ik} - \left(\bar{\partial}_j \tau_{ijk} \right) \right) = 0 \tag{3.7}$$

The *surface traction* t_k on the surface S of the body is

$$t_k = n_i \left(\sigma_{ik} - \left(\bar{\partial}_j \tau_{ijk} \right) \right) + n_i n_j \tau_{ijk} (D_p n_p) - D_j (n_i \tau_{ijk}) \tag{3.8}$$

and the *double-stress traction* r_k on S is

$$r_k = n_i n_j \tau_{ijk} \tag{3.9}$$

We conclude from (3.6) that the displacement field $\mathbf{u}$ must satisfy three equilibrium equations given by relation (3.7) and six boundary conditions given by (3.8) and (3.9).

For the special case where the surface S has edges, an additional term must be added to the right-hand side of (3.6). Suppose S has an edge C, formed by the intersection of two smooth surface segments $S^{(1)}$ and $S^{(2)}$ of S. The unit normal to segment $S^{(1)}$ is designated $\mathbf{n}^{(1)}$ and the unit normal to the segment $S^{(2)}$ is designated $\mathbf{n}^{(2)}$. The unit tangent $\mathbf{c}^{(1)}$ along the edge C is defined with segment $S^{(1)}$ to the left, and the unit tangent $\mathbf{c}^{(2)}$ is defined with segment $S^{(2)}$ to the left. We define the unit outward normal to C and lying within the surface $S^{(1)}$ by $\mathbf{k}^{(1)} = \mathbf{c}^{(1)} \times \mathbf{n}^{(1)}$; similarly, the unit outward normal to C and lying within $S^{(2)}$ is written as $\mathbf{k}^{(2)} = \mathbf{c}^{(2)} \times \mathbf{n}^{(2)}$. Then, the additional term to be added to the right-hand side of (3.6) upon application of the surface divergence theorem to (3.4) is

$$\int_C [p_k\, \delta u_k]\, ds^{(1)} \tag{3.10}$$

where $s^{(1)}$ is the arc length along the edge C in the direction $\mathbf{c}^{(1)}$. The line load p_k is given by

$$p_k = n_i^{(1)} k_j^{(1)} \tau_{ijk} - n_i^{(2)} k_j^{(2)} \tau_{ijk} \tag{3.11}$$

In the more general case, the piece-wise smooth surface S can be divided into a finite number of smooth parts, S_n, each bounded by an edge, C_n. The line-integral contribution (3.10) becomes

$$\sum_n \oint_{C_n} [p_k \, \delta u_k] \, ds \tag{3.12}$$

and the line load p_k along any sharp edges C_n is given by the jump in value Δ of $(n_i k_j \tau_{ijk})$ on each side of C_n:

$$p_k = \Delta(n_i k_j \tau_{ijk}) \tag{3.13}$$

The complete virtual work expression becomes

$$\int_V [\sigma_{ij} \, \delta \varepsilon_{ij} + \tau_{ijk} \, \delta \eta_{ijk}] \, dV = \int_V [f_k \, \delta u_k] \, dV + \int_S [t_k \, \delta u_k] \, dS + \int_S [r_k (D \, \delta u_k)] \, dS + \sum_n \oint_{C_n} [p_k \, \delta u_k] \, ds \tag{3.14}$$

Global equilibrium of forces dictates that the net force on the surface of the body vanishes. In order to obtain an explicit expression for the net force on the body we impose a uniform virtual displacement δu_i°. The associated internal work in (3.2) vanishes and the external work is given by

$$\delta w^{EXT} = \delta \mathbf{u}^\circ \cdot \int_S [\mathbf{n} \cdot (\boldsymbol{\sigma} - \bar{\boldsymbol{\partial}} \cdot \boldsymbol{\tau})] \, dS = 0 \tag{3.15}$$

Since this expression vanishes for all δu_i° we conclude that the net force on the body, given by $\int_S [n_i(\sigma_{ik} - \tau_{ijk,j})] \, dS$, vanishes. A similar argument is used to obtain an expression for the net moment on the body. For a body in equilibrium, the net moment on it vanishes, implying that the work done through an incremental displacement field $\delta \mathbf{u} = \delta \boldsymbol{\theta}^\circ \times \mathbf{x}$ vanishes for an arbitrary uniform rotation $\delta \boldsymbol{\theta}^\circ$. The internal virtual work vanishes

since a uniform rotation induces vanishing strains and vanishing strain gradient. The external work follows from (3.2) as

$$\delta w^{EXT} = \delta\boldsymbol{\theta}^{\circ} \cdot \int_S \left[\mathbf{x} \times \mathbf{n} \cdot (\boldsymbol{\sigma} - \bar{\partial} \cdot \boldsymbol{\tau}) + \frac{4}{3} \mathbf{n} \cdot \boldsymbol{\tau} : \mathbf{e} \right] dS = 0 \quad (3.16)$$

where $\mathbf{e}$ is the alternating tensor. Thus, the vanishing net moment on the body is the vector quantity working through $\delta\boldsymbol{\theta}^{\circ}$ in the equation above.

B. Connection with Couple Stress Theory

It is instructive to rearrange the principle of virtual work into a form which separates out the work terms associated with couple stresses and those associated with double forces per unit area. This decomposition leads to a transparent reduction of the general framework to couple stress theory when the constitutive behavior depends only on the rotation gradients. We shall consider first the general case of a compressive solid, and then specialize the results later for the incompressible limit.

Following the development of Smyshlyaev and Fleck (1996) the strain gradient tensor $\boldsymbol{\eta}$ is partitioned into a symmetric tensor $\boldsymbol{\eta}^S$ representing stretch gradients, and a curvature measure $\boldsymbol{\eta}^A$:

$$\boldsymbol{\eta} = \boldsymbol{\eta}^S + \boldsymbol{\eta}^A \quad (3.17)$$

In parallel with the definitions (2.10) and (2.11) for the deviatoric tensor $\boldsymbol{\eta}'$, we adopt the definitions

$$\eta^2_{ijk} \equiv \frac{1}{3}(\eta_{ijk} + \eta_{jki} + \eta_{kij}) \quad (3.18)$$

and

$$\eta^A_{ijk} \equiv \eta_{ijk} - \eta^S_{ijk} \equiv \frac{2}{3} e_{ikp} \chi_{pj} + \frac{2}{3} e_{jkp} \chi_{pi} \quad (3.19)$$

and note that η^S and η^A are orthogonal to one another. The $\eta^A - \chi$ relation may be inverted to give

$$\chi_{ij} = \frac{1}{2} e_{iqr} \eta^A_{jqr} \quad (3.20)$$

and so η^A is a useful third-order tensorial representation of the second-order curvature tensor. Each has eight independent components, since $\chi_{ii} = 0$.

A similar decomposition applies to the higher-order stress τ. We can split τ into a symmetric tensor τ^S defined by

$$\tau^S_{ijk} \equiv \frac{1}{3}(\tau_{ijk} + \tau_{jki} + \tau_{kij}) \tag{3.21}$$

and a remainder τ^A_{ijk} such that

$$\tau_{ijk} = \tau^S_{ijk} + \tau^A_{ijk} \tag{3.22}$$

On noting that τ^S is orthogonal to an arbitrary η^A and that τ^A_{ijk} is orthogonal to an arbitrary η^S the work increment δw can be written simply as

$$\delta w = \sigma_{ij}\,\delta\varepsilon_{ij} + \tau_{ijk}\,\delta\eta_{ijk} = \sigma_{ij}\,\delta\varepsilon_{ij} + \tau^S_{ijk}\,\delta\eta^S_{ijk} + \tau^A_{ijk}\,\delta\eta^A_{ijk} \tag{3.23}$$

The work term $\tau^A_{ijk}\,\delta\eta^A_{ijk}$ represents the work done by the couple stresses $\mathbf{m}$ acting through the curvature increment $\delta\boldsymbol{\chi}$,

$$\tau^A_{ijk}\,\delta\eta^A_{ijk} = m_{ji}\,\delta\chi_{ij} \tag{3.24}$$

On substituting (3.19) into (3.24) we obtain an explicit expression for $\mathbf{m}$ in terms of $\boldsymbol{\tau}^A$:

$$m_{jp} = \frac{4}{3}e_{ikp}\tau^A_{jik} = \frac{4}{3}e_{ikp}\tau_{jik} \tag{3.25}$$

and similarly, substitution of (3.20) into (3.24) gives the inversion formula

$$\tau^A_{jqr} = \frac{1}{4}e_{iqr}m_{ji} + \frac{1}{4}e_{ijr}m_{qi} \tag{3.26}$$

The higher-order stress terms $\boldsymbol{\tau}$ appearing in the reduced form of the principle of virtual work (3.14) can now be re-expressed in terms of couple stresses $\mathbf{m}$ and the symmetric tensor $\boldsymbol{\tau}^S$. The derivation is by successive application of Stoke's surface divergence theorem and follows that laid down by Toupin (1962) and Mindlin (1964). Here, we quote only the result:

$$\int_V \left[\sigma_{ij}\,\delta\varepsilon_{ij} + m_{ji}\,\delta\chi_{ij} + \tau^S_{ijk}\,\delta\eta^S_{ijk}\right] dV = \int_V [f_k\,\delta u_k]\,dV + \int_S [\bar{t}_k\,\delta u_k]\,dS$$

$$+ \int_S [\bar{q}_k\,\delta\theta_k]\,dS + \int_S [\bar{r}\,\delta\varepsilon_N]\,dS + \sum_n \oint_{C_n} [\bar{p}_k\,\delta u_k]\,ds \tag{3.27}$$

where the body forces f_k are in equilibrium with stresses within the volume V according to the relation (3.7), which may be rephrased as

$$\sigma_{ik,i} - \frac{1}{2}e_{jlk}m_{ij,il} - \tau^S_{ijk,ij} + f_k = 0 \tag{3.28}$$

The reduced surface traction $\bar{t}_k$ has three independent components which satisfy

$$\bar{t}_k = n_l\left(\sigma_{lk} - \frac{1}{2}m_{ij,i}e_{jlk} - \tau^S_{ilk,i}\right) - D_k\left[n_p\tau^S_{pkl}\right] - D_k\left[n_p n_s n_l \tau^S_{pks}\right]$$
$$+ n_k n_p \tau^S_{pkl}(D_j n_j) + n_k n_p n_s n_l \tau^S_{pks}(D_j n_j) \tag{3.29}$$

while the two reduced torque tractions $\bar{q}_k$ are tangential to the surface of the body and are given by

$$\bar{q}_k = n_i m_{ik} + 2n_i n_j n_p e_{kpq}\tau^S_{ijq} - n_k n_p\left(n_i m_{ip} + 2n_i n_j n_q e_{pqr}\tau^S_{ijr}\right) \tag{3.30}$$

The single double force $\bar{r}$ is the work conjugate to the normal strain increment $\delta\varepsilon_N \equiv n_i n_j\,\delta\varepsilon_{ij}$ and is related to $\boldsymbol{\tau}^S$ via

$$\bar{r} = n_i n_j n_k \tau^S_{ijk} \tag{3.31}$$

The line force $\bar{p}_k$ along the edges C_n of the piece-wise smooth surfaces S_n satisfies

$$\bar{p}_k = \Delta\left[n_i k_j \tau^S_{ijk} + n_i n_j n_k k_q \tau^S_{ijq} + \frac{1}{2}n_i n_p n_q k_r e_{qrk} m_{ip}\right] \tag{3.32}$$

The version (3.27–(3.32) of the principle of virtual work makes explicit the contribution to internal and external work from an increment in strain, an increment in rotation gradient (curvature) and an increment in stretch gradient. Following the argument of Koiter (1964), the spherical part of the couple stress tensor $\mathbf{m}$ enters neither the virtual work expression for the body nor the constitutive law (since $\boldsymbol{\chi}$ is a deviatoric tensor), and without loss of generality we may take $m_{ii} = 0$.

Now consider the limit when the strain energy density $\mathbf{w}$ depends only on strain and rotation gradients and has no dependence on $\boldsymbol{\eta}^S$. The double forces per unit area $\boldsymbol{\tau}^S$ vanish, the term $\int_S[\bar{r}\,\delta\varepsilon_N]\,dS$ in relation (3.27) disappears and the virtual-work expression reduces to that of couple-stress theory as given by (B15–B18) in Fleck *et al.* (1994)

C. The Incompressible Limit

In the incompressible limit, the mean stress σ_{ii} and the mean higher-order stress tensor τ^H do not appear in the constitutive law. We shall show that a consequence of the kinematic constraint imposed by incom-

pressibility is that the number of independent boundary conditions is reduced by one. Further, we may take τ^H to vanish identically without affecting any of the terms in the virtual work principle or constitutive law. The arguments are as follows.

Consider again the reduced form of the principle of virtual work for the compressible solid, as given by relation (3.13). Incompressibility places a kinematic restriction on the normal component of $D\,\delta u_i$ at the surface S of the body:

$$n_j D\,\delta u_j = -D_j\,\delta u_j \tag{3.33}$$

since

$$\bar{\partial}_j\,\delta u_j = D_j\,\delta u_j + n_j D\,\delta u_j = 0 \tag{3.34}$$

In other words, given a distribution of displacement increment δu_j on the surface of the body, the normal components $D\,\delta u_j$ are constrained by (3.33), and only the two tangential components of $D\,\delta u_j$ remain arbitrary. Consequently, only the two tangential components of the double-stress traction r_k can be specified as independent external tractions on the body. Somewhat lengthy manipulation of (3.14) and making use of (3.34) gives

$$\int_V [\sigma'_{ij}\,\delta\varepsilon'_{ij} + \tau'_{ijk}\,\delta\eta'_{ijk}]\,dV = \int_V [f_k\,\delta u_k]\,dV + \int_S [(\hat{t}_k + Hn_k)\,\delta u_k]\,dS + \int_S [\hat{r}_k(D\,\delta u_k)]\,dS + \sum_n \oint_{C_n} [\hat{p}_k\,\delta u_k]\,dS \tag{3.35}$$

where H is a combined measure of the hydrostatic stress according to

$$H \equiv \frac{1}{3}\sigma_{kk} - \frac{1}{2}\tau_{jkk,j} \tag{3.36}$$

The body force f_k is in equilibrium with the deviatoric stresses $(\boldsymbol{\sigma}', \boldsymbol{\tau}')$ and the distribution of H according to

$$f_k + \sigma'_{ik,i} - \tau'_{ijk,ij} + H_{,k} = 0 \tag{3.37}$$

The three independent surface tractions $\hat{t}_k$ on the surface S of the incompressible body are

$$\hat{t}_k = n_i(\sigma'_{ik} - \tau'_{ijk,j}) + D_k(n_i n_j n_p \tau'_{ijp}) - D_j(n_i \tau'_{ijk}) + [n_i n_j \tau'_{ijk} - n_k(n_i n_j n_p \tau'_{ijp})](D_q n_q) \tag{3.38}$$

and the *two* independent double-stress tractions $\hat{r}_k$ tangential to S are

$$\hat{r}_k = n_i n_j \tau'_{ijk} - n_i n_j n_p n_k \tau'_{ijp} \tag{3.39}$$

We emphasize that the constraint of material incompressibility has reduced the number of independent boundary conditions associated with the displacement gradient from three to two. The line load $\hat{p}_k$ in (3.35) is given by

$$\hat{p}_k = \Delta(n_i k_j \tau'_{ijk} - k_k n_i n_j n_p \tau'_{ijp}) \tag{3.40}$$

Note that the hydrostatic stress $\frac{1}{3}\sigma_{kk}$ and the hydrostatic higher stress τ^H enters the virtual work statement (3.35) only via the term in H appearing in the surface traction term of (3.35) and in the equilibrium statement (3.37). The relative magnitude of $\frac{1}{3}\sigma_{kk}$ and τ^H is arbitrary: only the combination H as defined in (3.36) is known. Therefore, we may simplify the virtual work statement by taking τ^H to vanish identically and put $\tau = \tau'$.

The number of independent boundary conditions in the alternative statement of virtual work (3.27) may similarly be reduced by one upon enforcing incompressibility. The incompressibility condition (3.33) implies that normal strain increment $\delta\varepsilon_N$ is not an independent kinematic quantity: it can be re-expressed in terms of direct strains tangential to the surface S. Thus, the term involving $\delta\varepsilon_N$ can be eliminated from (3.27) by making use of the identity

$$\int_S [\tilde{r}\,\delta\varepsilon_N]\,dS = \int_S \left[D_p\left(n_i n_j n_k \tau^S_{ijk}\right) - n_i n_j n_k n_p \tau^S_{ijk}(D_s n_s)\right] \delta u_p\,dS$$

$$- \sum_n \oint_{C_n} \left[\Delta\left(n_i n_j n_k k_p \tau^S_{ijk}\right) \delta u_p\right] ds \tag{3.41}$$

IV. Flow Theory

A flow theory version of strain gradient plasticity is now outlined, based on the physical argument that the current strength of the solid is dependent upon the accumulated strain and strain gradient. The resulting formulation results in a higher-order set of differential equations than conventional plasticity theory, with an associated increase in the number of boundary conditions. Consequently, the theory predicts the existence of

boundary layers of deformation near to stiff interfaces. An alternative strategy adopted by Bassani and co-workers (Acharya and Bassani, 1995) is to assume that the current tangent-hardening modulus is increased by the presence of accumulated strain gradients. The resulting formulation in rate form is then only a slight modification of conventional theory, with no additional boundary conditions, and no boundary layers near to interfaces. Additional experiments are required in order to determine which strategy is the more accurate. We believe the flow theory outlined below has a firm physical basis, and is consistent with the observed physical phenomena described in Section II.

In this section we first review conventional J_2 flow theory for an elastic-plastic solid. A strain gradient version of J_2 flow theory is then proposed, which is the complement to the deformation theory defined above. Stability and minimum principles follows in a straightforward fashion. Briefly, the strain gradient version of J_2 flow theory is generated by the following prescription. In the absence of higher-order stresses $\boldsymbol{\tau}$, the deviatoric, symmetric Cauchy stress $\boldsymbol{\sigma}'$ may be represented by a five-dimensional vector. When higher-order stresses are present the role of $\boldsymbol{\sigma}'$ is replaced by that of the 23-dimensional vector $\boldsymbol{\Sigma} \equiv (\boldsymbol{\sigma}', \boldsymbol{\tau}')$; $\boldsymbol{\Sigma}$ is made up of the five symmetric components of $\boldsymbol{\sigma}'$, the eight independent components of couple stress $\boldsymbol{\tau}'^{A}$ and the ten independent components of double force per unit area τ'^{S}. In like manner, the deviatoric strain tensor $\boldsymbol{\varepsilon}'$ is replaced by the 23-dimensional vector $\mathscr{E} \equiv (\boldsymbol{\varepsilon}', \boldsymbol{\eta}')$.

Review of conventional J_2 flow theory In conventional J_2 flow theory, higher-order stresses are absent and the strain tensor $\boldsymbol{\varepsilon}$ is decomposed additively into an elastic part $\boldsymbol{\varepsilon}^{\mathrm{el}}$ and a plastic part $\varepsilon^{\mathrm{pl}}$. The elastic strain is related to the Cauchy stress $\boldsymbol{\sigma}$ via the linear relation

$$\varepsilon_{ij}^{\mathrm{el}} = \mathscr{M}_{ijkl}\sigma_{kl} \tag{4.1a}$$

where

$$\mathscr{M}_{ijkl} = \frac{(1+\nu)}{2E}(\delta_{ik}\delta_{jl} + \delta_{il}\delta_{jk}) - \frac{\nu}{E}\delta_{ij}\delta_{kl} \tag{4.1b}$$

Here, E is Young's modulus and ν is Poisson's ratio.

The plasticity relations of conventional J_2 flow theory provide a connection between the plastic strain rate $\dot{\boldsymbol{\varepsilon}}^{\mathrm{pl}}$ and the stress rate $\dot{\boldsymbol{\sigma}}$: the plastic strain $\varepsilon^{\mathrm{pl}}$ is determined by integration of $\dot{\boldsymbol{\varepsilon}}^{\mathrm{pl}}$ with respect to time. In

J_2 theory, $\dot{\boldsymbol{\varepsilon}}^{\mathrm{pl}}$ is taken to be incompressible and the yield surface Φ is written as

$$\Phi(\boldsymbol{\sigma}, Y) = \sigma_e - Y = 0 \tag{4.2}$$

where σ_e is the von Mises effective stress, $\sigma_e \equiv \sqrt{\frac{3}{2} s_{ij} s_{ij}}$, and Y is the current flow stress. For a hardening solid, the material response is plastic when $\Phi = 0$ and $\dot{\sigma}_e > 0$; and the response is elastic when $\Phi < 0$, or $\Phi = 0$ and $\dot{\sigma}_e \leq 0$. The plastic strain rate $\dot{\boldsymbol{\varepsilon}}^{\mathrm{pl}}$ is assumed to be linear in the stress rate $\dot{\boldsymbol{\sigma}}$, and to lie normal to the current yield surface, giving

$$\dot{\boldsymbol{\varepsilon}}^{\mathrm{pl}} = \frac{1}{h(\sigma_e)} \frac{\partial \Phi}{\partial \boldsymbol{\sigma}} \dot{\sigma}_e \tag{4.3}$$

where the hardening rate h is chosen such that the uniaxial tensile response is reproduced. This dictates that h equals the tangent modulus of the stress versus plastic strain curve in simple tension. The work rate $\dot{U}$ per unit volume of the elastic-plastic body is

$$\dot{U} = \sigma_{ij} \dot{\varepsilon}_{ij} = \sigma_{ij} \dot{\varepsilon}_{ij}^{\mathrm{el}} + s_{ij} \dot{\varepsilon}_{ij}^{\mathrm{pl}} \tag{4.4}$$

and so $\dot{U}$ may be partitioned into an elastic part $\dot{U}^{\mathrm{el}} = \sigma_{ij} \dot{\varepsilon}_{ij}^{\mathrm{el}}$ and a plastic part $\dot{U}^{\mathrm{pl}} = s_{ij} \dot{\varepsilon}_{ij}^{\mathrm{pl}}$. Substitution of (4.3) into $\dot{U}^{\mathrm{pl}} = s_{ij} \dot{\varepsilon}_{ij}^{\mathrm{pl}}$ gives $\dot{U}^{\mathrm{pl}} = \sigma_e \dot{\sigma}_e / h$ which may be re-written as $\dot{U}^{\mathrm{pl}} = \sigma_e \dot{\varepsilon}_e^{\mathrm{pl}}$ where the effective plastic strain rate $\dot{\varepsilon}_e^{\mathrm{pl}} \equiv \dot{\sigma}_e / h$. Observe that $\dot{\varepsilon}_e^{\mathrm{pl}} = \sqrt{\frac{2}{3} \dot{\varepsilon}_{ij}^{\mathrm{pl}} \dot{\varepsilon}_{ij}^{\mathrm{pl}}}$ by direct evaluation, making use of (4.3).

Flow theory for strain gradient solid Now assume the existence of higher order stresses in the elastic-plastic body. We define the elastic strain energy density w^{el} for a purely elastic response of the isotropic, compressible solid by

$$\begin{aligned} W^{\mathrm{el}} = E\left(\frac{\nu}{2(1+\nu)(1-2\nu)} (\varepsilon_{kk}^{\mathrm{el}})^2 + \frac{1}{2(1+\nu)} \varepsilon_{ij}^{\mathrm{el}} \varepsilon_{ij}^{\mathrm{el}} \right) \\ + E\left(L_1^2 \eta_{ijk}^{\prime(1)} \eta_{ijk}^{\prime(1)} + L_2^2 \eta_{ijk}^{\prime(2)} \eta_{ijk}^{\prime(2)} + L_3^2 \eta_{ijk}^{\prime(3)} \eta_{ijk}^{\prime(3)} \right. \\ \left. + L_4^2 \eta_{ijk}^{H} \eta_{ijk}^{H} + L_5^2 \eta_{ijk}^{H} \eta_{kji}^{\prime(3)} \right) \end{aligned} \tag{4.5}$$

where the five elastic length scales L_n have no physical significance but are introduced in order to partition the strain gradient tensor $\boldsymbol{\eta}$ into an elastic part and a plastic part

$$\eta = \eta^{\mathrm{el}} + \eta^{\mathrm{pl}}. \tag{4.6}$$

It should be noted that the elastic part of the strain gradients cannot be expressed as gradients of the elastic strains alone when plastic strains occur. A sensible strategy is to take $L_n \ll \ell_n$ so that the dominant size effect is associated with plastic rather than elastic strain gradients. The elastic strain state $(\boldsymbol{\varepsilon}^{el}, \boldsymbol{\eta}^{el})$ is assumed to be related to the stress state $(\boldsymbol{\sigma}, \boldsymbol{\tau})$ via the elastic strain energy density w^{el}, giving

$$\boldsymbol{\sigma} = \mathscr{L} : \boldsymbol{\varepsilon}^{el} = \frac{\partial w^{el}}{\partial \boldsymbol{\varepsilon}^{el}} \tag{4.7}$$

and

$$\boldsymbol{\tau} = \mathscr{J} \vdots \boldsymbol{\eta}^{el} = \frac{\partial w^{el}}{\partial \boldsymbol{\eta}^{el}} \tag{4.8}$$

The elastic modulus $\mathscr{L}$ is the inverse of $\mathscr{M}$ defined in relation (4.1) above, and is given by

$$\mathscr{L}_{ijkl} = \frac{E}{2(1+\nu)}\left(\frac{2\nu}{1-2\nu}\,\delta_{ij}\delta_{kl} + \delta_{ik}\delta_{jl} + \delta_{il}\delta_{jk}\right) \tag{4.9}$$

An explicit expression for the elastic modulus $\mathscr{J}$ may be obtained by straightforward differentiation of (4.5) with respect to $\boldsymbol{\eta}^{el}$, respectively. However, the expression is lengthy and it is omitted here in the interests of brevity.

A prescription is now given for the dependence of the plastic-strain rate upon the stress rate in the presence of higher-order stresses. In the presence of higher-order stresses, the deviatoric, symmetric Cauchy stress $\boldsymbol{\sigma}'$ is replaced by the 23-dimensional vector $\Sigma = (\boldsymbol{\sigma}', \boldsymbol{\tau}')$ comprising the five components of $\boldsymbol{\sigma}'$ and the 18 components of $\boldsymbol{\tau}'$. Similarly, the plastic strain rate $\dot{\boldsymbol{\varepsilon}}^{pl}$ is replaced by the 23-dimensional vector $\dot{\mathscr{E}}^{pl} = (\dot{\boldsymbol{\varepsilon}}^{pl}, \dot{\boldsymbol{\eta}}^{pl})$. The yield surface (4.2) generalizes to

$$\Phi(\Sigma, Y) = \Sigma - Y = 0 \tag{4.10}$$

where the overall effective stress Σ is defined by

$$\Sigma^2 = \frac{3}{2}\sigma'_{ij}\sigma'_{ij} + \sum_{I=1}^{3}\left[\ell_I^{-2}\tau'^{(I)}_{ijk}\tau'^{(I)}_{ijk}\right] = \sigma_e^2 + \sum_{I=1}^{3}\left[\left(\frac{\tau_e^{(I)}}{\ell_I}\right)^2\right] \tag{4.11}$$

Here, σ_e is the usual von Mises effective stress,

$$\sigma_e = \sqrt{\frac{3}{2}\sigma'_{ij}\sigma'_{ij}} \tag{4.12}$$

and the higher-order effective stresses $\tau_e^{(\mathrm{I})}$ are defined by

$$\tau_e^{(\mathrm{I})} = \sqrt{\tau_{ijk}^{(\mathrm{I})}\tau_{ijk}^{(\mathrm{I})}} \qquad \text{(no sum on I)} \tag{4.13}$$

In a similar fashion, we introduce the effective plastic strain gradient rates $\dot{\eta}_e^{(\mathrm{I})^{\mathrm{pl}}}$ by

$$\dot{\eta}_e^{(\mathrm{I})^{\mathrm{pl}}} = \sqrt{\dot{\eta}_{ijk}^{(\mathrm{I})^{\mathrm{pl}}}\dot{\eta}_{ijl}^{(\mathrm{I})^{\mathrm{pl}}}} \qquad \text{(no sum on I)} \tag{4.14}$$

and an overall effective plastic strain rate $\dot{\mathscr{E}}^{\mathrm{pl}}$ by

$$\dot{\mathscr{E}}^{\mathrm{pl}} = \sqrt{\frac{2}{3}\dot{\varepsilon}_{ij}^{\mathrm{pl}}\dot{\varepsilon}_{ij}^{\mathrm{pl}} + \sum_{\mathrm{I}=1}^{3}\left[\ell_1^2\dot{\eta}_{ijk}^{(\mathrm{I})^{\mathrm{pl}}}\dot{\eta}_{ijk}^{(\mathrm{I})^{\mathrm{pl}}}\right]} \tag{4.15}$$

When the solid is subjected to a uniaxial tensile stress σ, $\Sigma = \sigma$ and yield occurs when $\sigma = Y$ by (4.10); we interpret Y as the uniaxial flow stress. Equation (4.10) is a natural generalization of (4.2) once it is assumed that σ' is replaced by $\Sigma = (\boldsymbol{\sigma}', \boldsymbol{\tau}')$ and σ_e by Σ in the higher-order version of the theory.

Plastic straining is assumed to be normal to the yield surface and the plastic-strain rate is taken to be linear in the stress rate: (4.3) then generalizes to

$$\dot{\mathscr{E}}^{\mathrm{pl}} = \frac{1}{h(\Sigma)}\frac{\partial \Phi}{\partial \Sigma}\dot{\Sigma} \tag{4.16}$$

where $\dot{\mathscr{E}}^{\mathrm{pl}} = (\dot{\boldsymbol{\varepsilon}}^{\mathrm{pl}}, \dot{\boldsymbol{\eta}}^{\mathrm{pl}})$ has already been defined. In the case of uniaxial tension, where the axial stress is σ and the plastic strain is $\varepsilon^{\mathrm{pl}}$, we find $\Sigma = \sigma$ and (4.16) reduces to

$$\dot{\varepsilon}^{\mathrm{pl}} = \frac{\dot{\sigma}}{h(\sigma)} \tag{4.17}$$

Thus, the interpretation of h remains the same as for conventional J_2 flow theory.

The plastic work rate $\dot{U}^{\mathrm{pl}}$ is, via (2.4),

$$\dot{\mathscr{E}}^{\mathrm{pl}} = \sqrt{\frac{2}{3}\dot{\varepsilon}_{ij}^{\mathrm{pl}}\dot{\varepsilon}_{ij}^{\mathrm{pl}} + \sum_{\mathrm{I}=1}^{3}\left[\ell_1^2\dot{\eta}_{ijk}^{(\mathrm{I})^{\mathrm{pl}}}\dot{\eta}_{ijk}^{(\mathrm{I})^{\mathrm{pl}}}\right]} \tag{4.18}$$

On substitution of the expression (4.16) for $\dot{\mathscr{E}}^{\mathrm{pl}}$ into (4.18) we get $\dot{U}^{\mathrm{pl}} = \Sigma\dot{\Sigma}/h$ which may be rewritten as $\dot{U}^{\mathrm{pl}} = \Sigma\dot{\mathscr{E}}^{\mathrm{pl}}$ where the overall effective plastic strain rate $\dot{\mathscr{E}}^{\mathrm{pl}} \equiv \dot{\Sigma}/h$.

A. Summary of Elastic-Plastic Constitutive Relations

The main constitutive relations in the strain gradient formulation are now summarized in index notation. Plastic flow is normal to the yield surface such that

$$\dot{\varepsilon}_{ij}^{\mathrm{pl}} = \frac{3}{2h}\frac{\sigma'_{ij}}{\Sigma}\dot{\Sigma} \tag{4.19a}$$

and

$$\dot{\eta}_{ijk}^{\mathrm{pl}} = \frac{\dot{\Sigma}}{h}\frac{\partial\Phi}{\partial\tau_{ijk}} = \frac{\dot{\Sigma}}{h\Sigma}\sum_{\mathrm{I}=1}^{3}\left[\ell_{\mathrm{I}}^{-2}\tau_{ijk}^{\prime(\mathrm{I})}\right] \tag{4.19b}$$

by (4.11) and (4.16). The rate of overall effective stress $\dot{\Sigma}$ is given by the rate form of (4.11),

$$\dot{\Sigma} = \frac{3}{2\Sigma}\sigma'_{ij}\dot{\sigma}'_{ij} + \frac{1}{\Sigma}\sum_{\mathrm{I}=1}^{3}\left[\ell_{\mathrm{I}}^{-2}\tau_{ijk}^{\prime(\mathrm{I})}\dot{\tau}_{ijk}^{\prime(\mathrm{I})}\right] \tag{4.19c}$$

The elastic strain rates follow from (4.1) and (4.8) as

$$\dot{\varepsilon}_{ij}^{\mathrm{el}} = \mathscr{M}_{ijkl}\dot{\sigma}_{kl} \tag{4.20}$$

and

$$\dot{\eta}_{ijk}^{\mathrm{el}} = \mathscr{K}_{ijklmn}\dot{\tau}_{lmn} \tag{4.21}$$

where $\mathbf{K} = \mathscr{L}^{-1}$. Note that the current formulation predicts that higher-order stresses remain present in the case of a purely elastic response with vanishing plastic strains. This is for purely mathematical convenience, and is given no physical significance. Indeed, the magnitude of the elastic higher-order stresses may be made arbitrarily small by choosing the ratio $L_{\mathrm{I}}/\ell_{\mathrm{I}}$ to be sufficiently small. In some cases it may even be convenient to

take L_I/ℓ_I to be on the order of unity (e.g. the cavitation problem in Section II.C.5). If the strain gradients are small in the elastic range, the choice of the L_I will hardly matter.

In the strain gradient versions above of J_2 deformation theory and J_2 flow theory, proportional loading occurs at a material point when all stress components of $(\boldsymbol{\sigma}, \boldsymbol{\tau})$ increase in fixed proportion. That is, with $(\boldsymbol{\sigma}^0, \boldsymbol{\tau}^0)$ fixed and λ as a monotonically increasing scalar quantity, the components $(\boldsymbol{\sigma}, \boldsymbol{\tau}) = \lambda(\boldsymbol{\sigma}^0, \boldsymbol{\tau}^0)$ increase proportionally. When proportional loading is experienced at a material point, it is readily shown that the predictions of the strain gradient versions above of J_2 deformation theory and J_2 flow theory coincide.

B. Minimum Principles

The yield surface (4.10) is convex in the stress space $(\boldsymbol{\sigma}, \boldsymbol{\tau})$ and the plastic strain rate is normal to the yield surface. Hence the strain gradient version of J_2 flow theory (with $h > 0$) satisfies the generalized Drucker's stability postulates (Drucker, 1951)

$$\dot{\sigma}_{ij}\dot{\varepsilon}^{\mathrm{pl}}_{ij} + \dot{\tau}_{ijk}\dot{\eta}^{\mathrm{pl}}_{ijk} \geq 0 \tag{4.22a}$$

for a stress rate $(\dot{\boldsymbol{\sigma}}, \dot{\boldsymbol{\tau}})$ corresponding to a plastic strain rate $(\dot{\boldsymbol{\varepsilon}}^{\mathrm{pl}}, \dot{\boldsymbol{\eta}}^{\mathrm{pl}})$, and

$$(\sigma_{ij} - \sigma^*_{ij})\dot{\varepsilon}^{\mathrm{pl}}_{ij} + (\tau_{ijk} - \tau^*_{ijk})\dot{\eta}^{\mathrm{pl}}_{ijk} \geq 0 \tag{4.22b}$$

for a stress state $(\boldsymbol{\sigma}, \boldsymbol{\tau})$ associated with a plastic strain rate $(\dot{\boldsymbol{\varepsilon}}^{\mathrm{pl}}, \dot{\boldsymbol{\eta}}^{\mathrm{pl}})$, and any other stress state $(\boldsymbol{\sigma}^*, \boldsymbol{\tau}^*)$ on or within the yield surface.

Minimum principles are now given for the displacement rate and for the stress rate, for the strain gradient version of J_2 flow theory. These minimum principles follow directly from those outlined by Koiter (1960) for phenomenological plasticity theories with multiple yield functions, and from the minimum principles given in more general form by Hill (1966) for a metal crystal deforming in multislip. The presence of higher-order stresses can be included simply by replacing $\boldsymbol{\sigma}'$ by $\boldsymbol{\Sigma}$ and $\dot{\boldsymbol{\varepsilon}}^{\mathrm{pl}}$ by $\dot{\mathscr{E}}^{\mathrm{pl}}$, as outlined above.

Consider a body of volume V and smooth surface S comprised of an elastic-plastic solid which obeys the strain gradient version of J_2 flow theory (4.19–4.21). The body is loaded by the instantaneous stress traction rate $\dot{t}^o_i$ and double stress traction rate $\dot{r}^o_i$ on a portion S_T of the surface

(see relations (3.6–3.9) for the definition of stress tractions and double stress tractions). The velocity is prescribed as $\dot{u}_i^o$ and the normal velocity gradient is prescribed as $D\dot{u}_i^o$ on the remaining portion S_u of the surface. Then the following minimum principles may be stated.

1. *Minimum Principle for the Displacement Rate*

Consider all admissible velocity fields $\dot{u}_i$ which satisfy $\dot{u}_i = \dot{u}_i^o$ and $D\dot{u}_i = D\dot{u}_i^o$ on S_u. Let $\dot{\varepsilon}_{ij} \equiv \frac{1}{2}(\dot{u}_{i,j} + \dot{u}_{j,i})$ and $\dot{\eta}_{ijk} = \dot{u}_{k,ij}$ be the state of strain rate derived from $\dot{u}_i$, and define $(\dot{\boldsymbol{\sigma}}, \dot{\boldsymbol{\tau}})$ to be the stress rate field associated with $(\dot{\boldsymbol{\varepsilon}}, \dot{\boldsymbol{\eta}})$ via the constitutive law for the strain-gradient version of J_2 flow theory (4.19–4.21) with a hardening modulus $h > 0$. Then, the functional $F(\dot{\mathbf{u}})$, defined by

$$F(\dot{\mathbf{u}}) = \frac{1}{2}\int_V \left[\dot{\sigma}_{ij}\dot{\varepsilon}_{ij} + \dot{\tau}_{ijk}\dot{\eta}_{ijk}\right] dV - \int_{S_T}\left[\dot{t}_i^o \dot{u}_i + \dot{r}_i^o D\dot{u}_i\right] dS \quad (4.23)$$

is minimized by the exact solution $(\dot{\mathbf{u}}, \dot{\boldsymbol{\varepsilon}}, \dot{\boldsymbol{\eta}}, \dot{\boldsymbol{\sigma}}, \dot{\boldsymbol{\tau}})$. The exact solution is unique since the minimum is absolute.

2. *Minimum Principle for the Stress Rate*

Consider instead all admissible equilibrium stress rate fields $(\dot{\boldsymbol{\sigma}}, \dot{\boldsymbol{\tau}})$ which satisfy the traction boundary conditions $\dot{t}_i = \dot{t}_i^o$ and $\dot{r}_i = \dot{r}_i^o$ on S_T. Let $\dot{u}_i^o$ and $D\dot{u}_i^o$ be prescribed on the remaining portion S_u, and define $(\dot{\boldsymbol{\varepsilon}}, \dot{\boldsymbol{\eta}})$ to be the state of strain rate associated with the stress rate $(\dot{\boldsymbol{\sigma}}, \dot{\boldsymbol{\tau}})$ via the constitutive law (4.19–4.21) with $h > 0$. Then, the functional $H(\dot{\boldsymbol{\sigma}}, \dot{\boldsymbol{\tau}})$, defined by,

$$H(\dot{\boldsymbol{\sigma}}, \dot{\boldsymbol{\tau}}) = \frac{1}{2}\int_V \left[\dot{\sigma}_{ij}\dot{\varepsilon}_{ij} + \dot{\tau}_{ijk}\dot{\eta}_{ijk}\right] dV - \int_{S_u}\left[\dot{t}_i \dot{u}_i^o + \dot{r}_i D\dot{u}_i^o\right] dS \quad (4.24)$$

is minimized by the exact solution $(\dot{\mathbf{u}}, \dot{\boldsymbol{\varepsilon}}, \dot{\boldsymbol{\eta}}, \dot{\boldsymbol{\sigma}}, \boldsymbol{\tau})$. Uniqueness follows directly from the statement that the minimum is absolute.

The proofs of the minimum principles for the displacement rate and stress rate require three fundamental inequalities, which are the direct extensions of those given by Koiter (1960) and Hill (1966), and are stated here without proof. Assume that at each material point a stress state $(\boldsymbol{\sigma}, \boldsymbol{\tau})$ is known; the material may, or may not, be at yield. Let $(\dot{\boldsymbol{\varepsilon}}, \dot{\boldsymbol{\eta}})$ be associated with any assumed $(\dot{\boldsymbol{\sigma}}, \dot{\boldsymbol{\tau}})$ via the constitutive law (4.19–4.21).

Similarly, let $(\dot{\boldsymbol{\varepsilon}}^*, \dot{\boldsymbol{\eta}}^*)$ be associated with an alternative stress rate field $(\dot{\boldsymbol{\sigma}}^*, \dot{\boldsymbol{\tau}}^*)$. Then, the three inequalities are

$$\left(\dot{\varepsilon}_{ij} - \dot{\varepsilon}^*_{ij}\right)\left(\dot{\sigma}_{ij} - \dot{\sigma}^*_{ij}\right) + \left(\dot{\eta}_{ijk} - \dot{\eta}^*_{ijk}\right)\left(\dot{\tau}_{ijk} - \dot{\tau}^*_{ijk}\right) \geq 0 \quad (4.25a)$$

$$\left(\dot{\varepsilon}^*_{ij}\dot{\sigma}^*_{ij} + \dot{\varepsilon}_{ij}\dot{\sigma}_{ij} - 2\dot{\varepsilon}^*_{ij}\dot{\sigma}_{ij}\right) + \left(\dot{\eta}^*_{ijk}\dot{\tau}^*_{ijk} + \dot{\eta}_{ijk}\dot{\tau}_{ijk} - 2\dot{\eta}^*_{ijk}\dot{\tau}_{ijk}\right) \geq 0 \quad (4.25b)$$

and

$$\left(\dot{\varepsilon}^*_{ij}\dot{\sigma}^*_{ij} + \dot{\varepsilon}_{ij}\dot{\sigma}_{ij} - 2\dot{\varepsilon}_{ij}\dot{\sigma}^*_{ij}\right) + \left(\dot{\eta}^*_{ijk}\dot{\tau}^*_{ijk} + \dot{\eta}_{ijk}\dot{\tau}_{ijk} - 2\dot{\eta}_{ijk}\dot{\tau}^*_{ijk}\right) \geq 0 \quad (4.25c)$$

The equality sign holds in the three expressions above if and only if $\dot{\boldsymbol{\sigma}}^* = \dot{\boldsymbol{\sigma}}$ and $\dot{\boldsymbol{\tau}}^* = \dot{\boldsymbol{\tau}}$.

V. Single-Crystal Plasticity Theory

We shall use the notions of statistically stored dislocations and geometrically necessary dislocations to provide the physical basis for continuum theory of single-crystal plasticity. Slip is assumed to occur on specific slip systems in a continuous manner. The increment in flow strength of any given slip system depends upon the rates of both the strain and the first spatial gradient of strain. The crystal theory fits within the framework of Toupin-Mindlin strain gradient theory described in Sections 3 and 4. It will be seen that the theory leads quite naturally to a dependence on gradients of rotation and stretch. Attention is restricted to the class of theories usually referred to as small strain theory for which it is tacitly assumed that stresses are small compared to the incremental moduli as well as small strains.

A. Kinematics

The relationship between plastic strain gradient and dislocation density in single crystals has been explored by Nye (1953) and Kroner (1958, 1961, 1962). We summarize the theory for the case of small deformations. In order to calculate the density of geometrically necessary dislocations, a crystal lattice is embedded within the solid. We assume that the material shears through the crystal lattice by dislocation motion, and that the lattice (and attached material) undergoes rotation and elastic stretching as shown

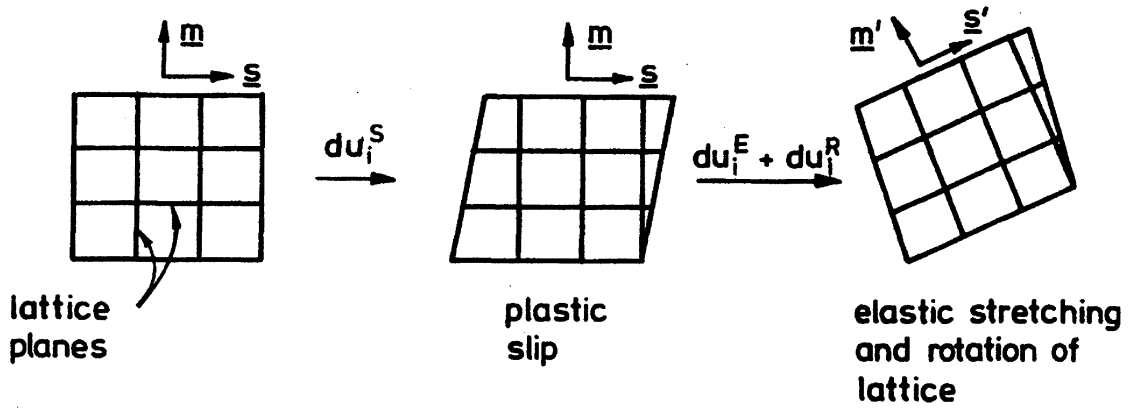

FIG. 14. The elastic-plastic deformation of a single crystal. Here, du_i^S is illustrated for single slip which in the text du_i^S is defined for the general case of multi-slip.

in Figure 14. Consider the relative displacement du_i of two material points separated by dx_j, in a Cartesian reference frame. The relative displacement du_i is decomposed into a displacement du_i^S due to slip, a displacement du_i^R due to rotation, and a displacement du_i^E due to elastic stretching,

$$du_i = du_i^S + du_i^R + du_i^E \tag{5.1a}$$

where

$$du_i^S \equiv \gamma_{ij}\, dx_j \tag{5.1b}$$

$$du_i^R \equiv \phi_{ij}\, dx_j \tag{5.1c}$$

and

$$du_i^E = \varepsilon_{ij}^{\mathrm{el}}\, dx_j \tag{5.1d}$$

Here, du_i^S is linearly related to dx_j via the *slip tensor* γ_{ij}, du_i^R is related to dx_j via the *lattice rotation tensor* ϕ_{ij}, and du_i^E is related to dx_j via the *elastic strain tensor* $\varepsilon_{ij}^{\mathrm{el}}$.

A particular slip system, α, is specified by the vectors $(\mathbf{s}^{(\alpha)}, \mathbf{m}^{(\alpha)})$ where $s^{(\alpha)}$ is the slip direction and $\mathbf{m}^{(\alpha)}$ is the slip plane normal. The slip tensor γ_{ij} is associated with an amount of slip $\gamma^{(\alpha)}$ on each of the slip systems, hence

$$\gamma_{ij} = \sum_{\alpha} \gamma^{(\alpha)} s_i^{(\alpha)} m_j^{(\alpha)} \tag{5.2}$$

where the summation is taken over all slip systems. The total strain $\varepsilon_{ij} = \frac{1}{2}(u_{i,j} + u_{j,i})$ at a material point equals the sum of the elastic strain

ε_{ij}^{el} and the plastic strain ε_{ij}^{pl}, where ε_{ij}^{pl} is the symmetric part of γ_{ij} such that

$$\varepsilon_{ij}^{pl} = \frac{1}{2}(\gamma_{ij} + \gamma_{ji}) = \sum_{\alpha} \gamma^{(\alpha)} \mu_{ij}^{(\alpha)} \tag{5.3a}$$

where

$$\mu_{ij}^{(\alpha)} \equiv \frac{1}{2}\left(s_i^{(\alpha)} m_j^{(\alpha)} + s_j^{(\alpha)} m_i^{(\alpha)}\right) \tag{5.3b}$$

The density of geometrically necessary dislocations is related to the net Burger's vector B_i associated with crystallographic slip. Make an imaginary cut in the crystal in order to produce a surface S of outward normal $\mathbf{n}$. Define B_i as the resulting displacement discontinuity due to slip on completion of a Burger's circuit around the periphery Γ of the surface S. In other words, B_i completes the circuit when Γ is traversed in the sense of a right-handed screw motion along $\mathbf{n}$. Thus, B_i is

$$B_i = \oint_{\Gamma} du_i^S = \oint_{\Gamma} \gamma_{ij}\, dx_j \tag{5.4}$$

which may be rewritten using Stokes's theorem as

$$B_i = \int_S \alpha_{in} n_n\, dS \tag{5.5}$$

where

$$\alpha_{in} = e_{nkj} \gamma_{ij,k} \tag{5.6}$$

In (5.6) e_{nkj} denotes the alternative tensor. The tensor α is Nye's *dislocation density tensor* or torsion-flexure tensor. It gives a direct measure of the number of geometrically necessary dislocations. Kroner's $\boldsymbol{\alpha}$ tensor, here labelled $\boldsymbol{\alpha}_K$, is related to Nye's tensor $\boldsymbol{\alpha}$ by $\boldsymbol{\alpha}_K = -\boldsymbol{\alpha}^T$, where the superscript T denotes the transpose. Nye (1953) has related $\boldsymbol{\alpha}$ to the distribution of individual dislocations within a crystal as follows. Suppose there exist dislocations parallel to the unit vector $\mathbf{r}$ with Burger's vector $\mathbf{b}$. Let there be N of these dislocations crossing unit area normal to $\mathbf{r}$. The number crossing a unit area normal to the unit vector $\mathbf{n}$ is $N\mathbf{n} \cdot \mathbf{r}$, and the associated Burger's vector is $N(\mathbf{n} \cdot \mathbf{r})\mathbf{b}$. Hence in suffix notation $B_i = Nn_j r_j b_i$ and from (5.5),

$$\alpha_{ij} = N b_i r_j \tag{5.7}$$

If there are other sets of dislocations present with different values of N, $\mathbf{b}$, and $\mathbf{r}$, then the total α_{ij} is obtained by summing the values of $Nb_i r_j$ from each set.

It must be emphasized that, if the distribution of dislocations is continuous, the net displacement discontinuity,

$$\oint du_i,$$

vanishes along any closed path within the material, because the incompatibility in displacement

$$B_i = \oint du_i^S$$

due to slip is exactly matched by an equal and opposite displacement mismatch

$$\oint (du_i^R + du_i^E),$$

as demanded by (5.1a). It is clear from (5.1a) and (5.5–5.7) that the density of geometrically necessary dislocations is defined unambiguously only when a crystal structure is embedded in the material. We treat α_{ij} as the fundamental measure of the total density of geometrically necessary dislocations.

An alternative version of the expression (5.6) for α_{ij} may be derived through introduction of the unit vector $\mathbf{t} \equiv \mathbf{s} \times \mathbf{m}$. Note that $(\mathbf{s}, \mathbf{m}, \mathbf{t})$ forms a right-handed triad with $\mathbf{t}$ in the slip plane and orthogonal to $\mathbf{s}$. Substitution of the relation $\mathbf{m} = \mathbf{t} \times \mathbf{s}$ into (5.2) gives via (5.6)

$$\alpha_{in} = \sum_{\alpha} s_i^{(\alpha)} \gamma_{,k}^{(\alpha)} (s_k^{(\alpha)} t_n^{(\alpha)} - t_k^{(\alpha)} s_n^{(\alpha)}) \tag{5.8}$$

The dependence of $\boldsymbol{\alpha}$ upon the slip gradient in the slip direction $\mathbf{s}$, and in the transverse direction $\mathbf{t}$ is made explicit by (5.8). (A slip gradient in the slip direction $\mathbf{s}$ is associated with edge dislocations lying along the $\mathbf{t}$ direction with Burger's vector parallel to the $\mathbf{s}$ direction. Similarly, a slip gradient in the $\mathbf{t}$ direction is associated with screw dislocations lying along the $\mathbf{s}$ direction and Burger's vector parallel to the $\mathbf{s}$ direction.) Note that a slip gradient in the $\mathbf{m}$ direction does not contribute to $\boldsymbol{\alpha}$, as shown explicitly by relation (5.8).

The strain gradient $\eta_{jki} \equiv u_{i,jk}$ is related to the slip tensor γ_{ij}, lattice rotation tensor ϕ_{ij} and elastic strain tensor ε_{ij}^{el} by differentiating (5.1) with respect to x_k to give

$$\eta_{jki} \equiv u_{i,jk} = \gamma_{ij,k} + \phi_{ij,k} + \varepsilon_{ij,k}^{el} \tag{5.9}$$

This expression for η can be simplified by using compatibility to eliminate the term $\phi_{ij,k}$ as follows. First, the lattice rotation tensor ϕ_{ij} is rewritten in term of the lattice rotation vector θ_k as $\phi_{ij} = e_{kji}\theta_k$. By continuity of displacement $e_{pjk}\eta_{jki} = e_{pjk}u_{i,jk}$ vanishes, and thus (5.9) reduces to

$$e_{pjk}\gamma_{ik,j} + e_{pjk}e_{ilk}\theta_{l,j} + e_{pjk}\varepsilon_{ik,j}^{el} = 0 \tag{5.10}$$

This relation may be inverted to give

$$\theta_{p,i} = e_{pjk}\gamma_{ik,j} - \frac{1}{2}\delta_{pi}e_{sjk}\gamma_{sk,j} + e_{pjk}\varepsilon_{ik,j}^{el} \tag{5.11}$$

and (5.9) can thereby be rewritten as

$$\eta_{jki} = \gamma_{ik,j} + \gamma_{ji,k} - \gamma_{jk,i} - \frac{1}{2}e_{jki}e_{spq}\gamma_{sq,p} + \varepsilon_{ij,k}^{el} - \varepsilon_{jk,i}^{el} + \varepsilon_{ik,j}^{el} \tag{5.12}$$

The strain gradient tensor $\boldsymbol{\eta}$ may now be decomposed additively into an elastic part $\boldsymbol{\eta}^{el}$ and a plastic part $\boldsymbol{\eta}^{pl}$ as

$$\eta_{jki}^{el} = \varepsilon_{ij,k}^{el} - \varepsilon_{jk,i}^{el} + \varepsilon_{ik,j}^{el} \tag{5.13a}$$

and

$$\eta_{jki}^{pl} = \gamma_{ik,j} + \gamma_{ji,k} - \gamma_{jk,i} - \frac{1}{2}e_{jki}e_{spq}\gamma_{sq,p} \tag{5.13b}$$

We note in passing that the lattice curvature $\theta_{p,i}$ is closely connected to Nye's measure of the total density of geometrically necessary dislocations, α_{ij}: upon making use of (5.6), the relation (5.11) can be re-expressed as

$$\theta_{i,j} = \alpha_{ji} - \frac{1}{2}\delta_{ij}\alpha_{kk} + e_{ikl}\varepsilon_{jl,k}^{el} \tag{5.14}$$

The plastic strain gradient η_{jki}^{pl} can be expressed in terms of the sum of the gradient slip over N slip planes as

$$\eta_{ijk}^{pl} = \sum_{\alpha} \gamma_{,p}^{(\alpha)}\psi_{pijk}^{(\alpha)} \tag{5.15}$$

where the resolution tensor $\boldsymbol{\psi}$ is given by

$$\psi_{pijk}^{(\alpha)} \equiv \delta_{pi} s_k^{(\alpha)} m_j^{(\alpha)} + \delta_{pj} s_i^{(\alpha)} m_k^{(\alpha)} - \delta_{pk} s_i^{(\alpha)} m_j^{(\alpha)} + \frac{1}{2} t_p^{(\alpha)} e_{ijk} \quad \text{(no sum on } \alpha\text{)} \tag{5.16}$$

B. Stress Measures for Activating Slip

We employ a work statement in order to define the appropriate stress measures to activate yield on any slip system α. With the work conjugate of the slip rate $\dot{\gamma}^{(\alpha)}$ as $\tau^{(\alpha)}$ and the work conjugate of the gradient of slip rate $\dot{\gamma}_{,p}^{(\alpha)}$ as $Q_p^{(\alpha)}$, the plastic work rate per unit volume $\dot{w}^{\mathrm{pl}}$ over the active slip systems is

$$\dot{w}^{\mathrm{pl}} = \sum_{\alpha} \left[\tau^{(\alpha)} \dot{\gamma}^{(\alpha)} + Q_p^{(\alpha)} \dot{\gamma}_{,p}^{(\alpha)} \right] \tag{5.17}$$

In terms of macroscopic quantities, the internal plastic work rate follows from (2.4) as

$$\dot{w}^{\mathrm{pl}} = \sigma_{ij} \dot{\varepsilon}_{ij}^{\mathrm{pl}} + \tau_{ijk} \dot{\eta}_{ijk}^{\mathrm{pl}} \tag{5.18}$$

where $\dot{\varepsilon}_{ij}^{\mathrm{pl}}$ and $\dot{\eta}_{ijk}^{\mathrm{pl}}$ denote the plastic part of the strain rate $\dot{\varepsilon}_{ij}$ and strain rate gradient $\dot{\eta}_{ijk}$, respectively. On equating the two expressions above for the plastic work rate for arbitrary $\dot{\gamma}^{(\alpha)}$ and $\dot{\gamma}_{,p}^{(\alpha)}$, we obtain explicit expressions for $\tau^{(\alpha)}$ and via (5.3 and 5.15),

$$\tau^{(\alpha)} = \mu_{ij}^{(\alpha)} \sigma_{ij} \tag{5.19}$$

and

$$Q_p^{(\alpha)} = \psi_{pijk}^{(\alpha)} \tau_{ijk} \tag{5.20}$$

We note from (5.19) that the work conjugate of the slip rate $\dot{\gamma}^{(\alpha)}$ is the resolved shear stress $\tau^{(\alpha)}$ on the slip plane and in the slip direction. In similar fashion, the work conjugate of the gradient of slip rate $\dot{\gamma}_{,p}^{(\alpha)}$ is the resolved double force per unit area $Q_p^{(\alpha)}$ on the slip plane. We adopt the notation that the slip gradient along the slip direction $\mathbf{s}^{(\alpha)}$ is $\dot{\gamma}_{,S}^{(\alpha)}$, the slip gradient along the normal $\mathbf{m}^{(\alpha)}$ to the slip plane (α) is $\dot{\gamma}_{,M}^{(\alpha)}$, and the slip gradient along the transverse direction $\mathbf{t}^{(\alpha)} = \mathbf{s}^{(\alpha)} \times \mathbf{m}^{(\alpha)}$ to the slip plane

α is $\dot{\gamma}_{,T}^{(\alpha)}$. Then, upon substituting (5.16) into (5.20), the work conjugates to $\dot{\gamma}_{,S}^{(\alpha)}$, $\dot{\gamma}_{,M}^{(\alpha)}$ and $\dot{\gamma}_{,T}^{(\alpha)}$ are

$$Q_s^{(\alpha)} = s_i^{(\alpha)} s_j^{(\alpha)} m_k^{(\alpha)} \tau_{ijk} \tag{5.21a}$$

$$Q_M^{(\alpha)} = m_i^{(\alpha)} m_j^{(\alpha)} s_k^{(\alpha)} \tau_{ijk} \tag{5.21b}$$

and

$$Q_T^{(\alpha)} = \left(t_i^{(\alpha)} m_j^{(\alpha)} s_k^{(\alpha)} + s_i^{(\alpha)} t_j^{(\alpha)} m_k^{(\alpha)} - s_i^{(\alpha)} m_j^{(\alpha)} t_k^{(\alpha)} \right) \tau_{ijk} \tag{5.21c}$$

respectively, with no sum on α in the expressions above.

The notation of statistically stored and geometrically necessary dislocations suggests that the amount of strain hardening of a slip system is governed by the accumulated slip and the accumulated slip gradient on that slip system (and on all slip systems if latent hardening is taken into account). By analogy with the classical theory, we assume that yield of a given slip system (α) occurs when some combination of the resolved stress-like quantities $\tau^{(\alpha)}$, $Q_S^{(\alpha)}$, $Q_M^{(\alpha)}$, and $Q_T^{(\alpha)}$ attains a critical value. The precise details of the formulation are not yet clear but are being pursued.

Appendix. J_2 Deformation Theory and Associated Minimum Principles

We begin by writing the effective stress Σ as the work conjugate of $\mathscr{E}$, with

$$\Sigma = \frac{dw(\mathscr{E})}{d\mathscr{E}} \tag{A1}$$

With the particular choice for $w(\mathscr{E})$ given by (2.21) note that Σ is a power law function of $\mathscr{E}$:

$$\Sigma = \Sigma_0 \left(\frac{\mathscr{E}}{\mathscr{E}_0} \right)^{1/n} \tag{A2}$$

Assume the solid is incompressible and can support Cauchy stress, couple stresses and double stresses. Then, the work done per unit volume equals the increment in strain energy,

$$\delta w = \sigma'_{ij} \, \delta \varepsilon'_{ij} + \tau'_{ijk} \, \delta \eta'_{ijk} \tag{A3}$$

where the primes denote deviatoric measures. The work relation above and the definition (2.15) enables us to write the deviatoric stress $(\boldsymbol{\sigma}', \boldsymbol{\tau}')$ in terms of the strain state of the solid as

$$\delta'_{ij} = \frac{\partial w}{\partial \varepsilon'_{ij}} = \Sigma \frac{\partial \mathscr{E}}{\partial \varepsilon'_{ij}} = \frac{2}{3} \frac{\Sigma}{\mathscr{E}} \varepsilon'_{ij} \tag{A4}$$

and

$$\tau'_{ijk} = \frac{\partial w}{\partial \eta'_{ijk}} = \Sigma \frac{\partial \mathscr{E}}{\partial \eta'_{ijk}} = \sum_{I=1}^{3} \tau'^{(I)}_{ijk} \tag{A5a}$$

where

$$\tau'^{(I)}_{ijk} \equiv \frac{\Sigma}{\mathscr{E}} \ell_I^2 \eta'^{(I)}_{ijk} \qquad \text{(no sum on I)} \tag{A5b}$$

Note that the three stress measures $\tau'^{(I)}_{ijk}$ are the unique orthogonal decomposition of τ'_{ijk}, and they are the work conjugates to the three-strain gradient measures $\eta'^{(I)}_{ijk}$, giving

$$\delta w = \sigma'_{ij}\, \delta \varepsilon'_{ij} + \sum_{I=1}^{3} \left[\tau'^{(I)}_{ijk}\, \delta \eta'^{(I)}_{ijk} \right] \tag{A6}$$

An explicit formula for the overall effective stress measure Σ is derived by substituting (A4–A5) into (2.15), viz

$$\Sigma^2 = \tfrac{3}{2} \sigma'_{ij} \sigma'_{ij} + \sum_{I=1}^{3} \left[\ell_I^{-2} \tau'^{(I)}_{ijk} \tau'^{(I)}_{ijk} \right] \tag{A7}$$

Minimum Principles Principles of minimum potential energy and minimum complementary energy can be written in a straightforward manner. The proofs are omitted as they follow immediately the development of Fleck and Hutchinson (1993) for the non-linear couple stress solid.

Consider a body of volume V and surface S comprised of the non-linear strain gradient solid. In general the solid may be taken as compressible. A stress traction t_k^o and a double-stress traction r_k^o act on a portion S_T of the surface of the body. (Recall the relation between surface tractions and stresses given in (3.8) and (3.9).) Body forces are neglected in the current development. On the remaining portion S_u of the surface the displacement is prescribed as u_k^o and the gradient of displacement normal to the surface is prescribed as Du_k^o. Then, the following minimum principles may be stated.

Principle of minimum potential energy Consider all admissible displacement fields u_i which satisfy $u_i = u_i^o$ and $Du_k = Du_k^o$ on a part of the boundary S_u. Let $\varepsilon_{ij} = \frac{1}{2}(u_{i,j} + u_{j,i})$ and $\eta_{ijk} = u_{k,ij}$ be the strain state derived from u_i, and take $(\boldsymbol{\sigma}, \boldsymbol{\tau})$ to be the stress field associated with $(\boldsymbol{\varepsilon}, \boldsymbol{\eta})$ via $\sigma_{ij} = \partial w/\partial \varepsilon_{ij}$ and $\tau_{ijk} = \partial w/\partial \eta_{ijk}$. Define the potential energy $P(\mathbf{u})$ as

$$P(\mathbf{u}) = \int_V w(\boldsymbol{\varepsilon}, \boldsymbol{\eta})\, dV - \int_{S_T} [t_i^o u_i + r_i^o Du_i]\, dS \tag{A8}$$

where the surface integral is taken over that part S_T of the surface of the body over which the loading t_k^o and r_k^o are prescribed. Regard $P(\mathbf{u})$ as a functional in the class of kinematically admissible displacement fields $\mathbf{u}$. *Then, provided w is strictly convex in $\boldsymbol{\varepsilon}$ and $\boldsymbol{\eta}$, the potential energy $P(\mathbf{u})$ attains an absolute minimum for the actual displacement field.*

For the constitutive law described by (2.15) and (2.21) w is convex in $(\boldsymbol{\varepsilon}, \boldsymbol{\eta})$ and the potential energy (A8) is minimized by the actual displacement field.

Principle of minimum complementary energy In order to develop a minimum principle for the complementary energy it is necessary to introduce the stress potential $\phi(\boldsymbol{\sigma}, \boldsymbol{\tau})$ which is the dual of $w(\boldsymbol{\varepsilon}, \boldsymbol{\eta})$,

$$\begin{aligned}\phi(\boldsymbol{\sigma}, \boldsymbol{\tau}) &= \int_0^{\sigma} \varepsilon_{ij}\, d\sigma_{ij} + \int_0^{\tau} \eta_{ijk}\, d\tau_{ijk} = \sigma_{ij}\varepsilon_{ij} + \tau_{ijk}\eta_{ijk} - w(\boldsymbol{\varepsilon}, \boldsymbol{\eta}) \\ &= \frac{\Sigma_0 \mathscr{E}_0}{n+1}\left(\frac{\Sigma}{\Sigma_0}\right)^{n+1}\end{aligned} \tag{A9}$$

Thus the strain state $(\boldsymbol{\varepsilon}, \boldsymbol{\eta})$ is derived from the stress state $(\boldsymbol{\sigma}, \boldsymbol{\tau})$ via $\varepsilon_{ij} = \partial\phi/\partial\sigma_{ij}$ and $\eta_{ijk} = \partial\phi/\partial\tau_{ijk}$.

Define the complementary energy $C(\boldsymbol{\sigma}, \boldsymbol{\tau})$ as

$$C(\boldsymbol{\sigma}, \boldsymbol{\tau}) = \int_V \phi(\boldsymbol{\sigma}, \boldsymbol{\tau})\, dV - \int_{S_u} [t_i u_i^o + r_i Du_i^o]\, dS \tag{A10}$$

and consider all admissible equilibrium stress states $(\boldsymbol{\sigma}, \boldsymbol{\tau})$ which satisfy the traction boundary conditions $t_i = t_i^o$ and $r_i = r_i^o$ on S_T. Let u_i^o and Du_i^o be prescribed on the remaining portion S_u, and define $(\boldsymbol{\epsilon}, \boldsymbol{\eta})$ as the state of strain associated with the stress $(\boldsymbol{\sigma}, \boldsymbol{\tau})$ via $\varepsilon_{ij} = \partial\phi/\partial\sigma_{ij}$ and $\eta_{ijk} = \partial\phi/\partial\tau_{ijk}$. *Then, provided ϕ is strictly convex in $(\boldsymbol{\sigma}, \boldsymbol{\tau})$, the complementary energy $C(\boldsymbol{\sigma}, \boldsymbol{\tau})$ attains an absolute minimum for the actual stress field.*

Acknowledgments

The authors are grateful for many helpful discussions with Profs. M. F. Ashby and A. G. Evans, and for insightful comments by Dr. V. P. Smyshlyaev. The work of NAF was supported by grant N00014-92-J-1916 and N00014-92-J-1960 from the U.S. Office of Naval Research. The work of J. W. H. was supported in part by grants N00014-92-J-1960 from the U.S. Office of Naval Research and MSS-92-02141 from the National Science Foundation, and in part by the Division of Applied Sciences, Harvard University.

References

Acharya, A., and Bassani, J. L. (1995). On non-local flow theories that preserve the classical structure of incremental boundary value problems. *In* "Micromechanics of Plasticity and Damage of Multiphase Materials," IUTAM Symposium, Paris, Aug. 29–Sept. 1, 1995.

Aifantis, E. C. (1984). On the microstructural origin of certain inelastic models. *Trans. ASME J. Eng. Mater. Technol.* **106**, 326–330.

Ashby, M. F. (1970). The deformation of plastically non-homogeneous alloys. *Philos. Mag.* **21**, 399–424.

Ashby, M. F. (1971). The deformation of plastically non-homogeneous alloys. "Strengthening Methods in Crystals" (A. Kelly and R. B. Nicholson, eds.), Chapter 3, pp. 137–192. Elsevier, Amsterdam.

Bagchi, A., and Evans, A. G. (1996). The mechanics and physics of thin film decohesion and its measurement. *Interface Science* **3**, 169–193.

Bao, G., Hutchinson, J. W., and McMeeking, R. M. (1991). Particle reinforcement of ductile matrices against plastic flow and creep. *Acta Metall. Mater.* **39**, 1871–1882.

Bardenhagen, S., and Triantafyllidis, N. (1996). The influence of scale size on the stability of periodic solids and the role of associated higher order gradient continuum models. *J. Mech. Phys. Solids* in press.

Basinski, S. J., and Basinski, Z. S. (1966). Chapter 1, The nature of the cold worked state. *Recrystallization, Grain Growth and Textures, A.S.M.*, 1–44.

Bishop, R. F., Hill, R., and Mott, N. F. (1945). The theory of indentation and hardness tests. *Proc. Phys. Soc.* **57**(3), 147–159.

Bower, A. F., Fleck, N. A., Needleman, A., and Ogbonna, N. (1993). Indentation of a power law creeping solid. *Proc. R. Soc. London* **441**, 97–124.

Brown, L. M., and Stobbs, W. M. (1976). The work hardening of copper-silica. V Equilibrium plastic relaxation by secondary dislocations. *Philos. Mag.* **34**(3), 351–372.

Budiansky, B. (1959). A reassessment of deformation theories of plasticity. *J. Appl. Mech.* **26**, 259–264.

de Borst, R. (1993). A generalization of J_2-flow theory for polar continua. *Computer Methods in Applied Mechanics and Engineering* **103**, 347–362.

Drucker, D. C. (1951). A more fundamental approach to plastic stress-strain relations. *Proc. 1st U.S. Natl. Congr. Appl. Mech., ASME*, 487–491.

Drugan, W. J., and Willis, J. R. (1996). A micromechanics-based nonlocal constitutive equation and estimates of representative volume element size for elastic composites. *J. Mech. Phys. Solids* **44**, 497–524.

Eringen, A. C. (1968). Theory of micropolar elasticity. *In* "Fracture, An Advanced Treatise" (H. Liebowitz, ed.), Vol. 2, chapter 7, pp. 621–729. Academic Press, New York.

Essmann, U., Rapp. M., and Wilkins, M. (1968). Die versetzungsanordnung in plastisch verformten kupfervielkristallen. *Acta Metall.* **16**, 1275–1287.

Fleck, N. A., and Hutchinson, J. W. (1993). A phenomenological theory for strain gradient effects in plasticity. *J. Mech. Phys. Solid* **41**(12), 1825–1857.

Fleck, N. A., Muller, G. M., Ashby, M. F., and Hutchinson, J. W. (1994). Strain gradient plasticity: Theory and experiment. *Acta Metall. Mater.* **42**(2), 475.

Funkenbusch, P. D., and Courtney, T. H. (1985). On the strength of heavily cold worked *in situ* composites. *Acta Metall.* **33**(5), 913–922.

Funkenbusch, P. D., Lee, J. K., and Courtney, T. H. (1987). Ductile two-phase alloys: Prediction of strengthening at high strains. *Metall. Trans. A* **18A**, 1249–1256.

Gologanu, M., Leblond, J.-B., and Perrin, G. (1995). A micromechanically based Gurson-type model for ductile porous metals including strain gradient effects. "Net Shape Processing of Powder Materials" (S. Krishnaswami, R. M. McMeeking, and J. R. L. Trasorras, eds.), *ASME AMD* Vol. 216, pp. 47–56. American Society of Mechanical Engineering, New York.

Gurson, A. L. (1977). Continuum theory of ductile rupture by void nucleation and growth: part I—yield criteria and flow rules for porous ductile media. *J. Eng. Mater. Technol.* **99**, 2–15.

Hill, R. (1966). Generalized constitutive relations for incremental deformation of metal crystals by multislip. *J. Mech. Phys. Solids* **14**, 95–102.

Huang, Y., Hutchinson, J. W., and Tvergaard, V. (1991). Cavitation instabilities in elastic-plastic solids. *J. Mech. Phys. Solids* **39**(2), 223–241.

Huang, Y., Zhang, L., Guo, T. F., and Hwang, K. C. (1995). Near-tip fields for cracks in materials with strain gradient effects. To be published in the IUTAM Proceedings of a meeting on Nonlinear Fracture Mechanics (J. R. Willis, ed.), September, 1995, Cambridge.

Kakunai, S., Masaki, J., Kuroda, R., Iwata, K., and Nagata, R. (1985). Measurement of apparent Young's modulus in the bending of cantilever beam by heterodyne holographic interferometry. *Exp. Mech.*, 408–412.

Koiter, W. T. (1960). General theorems for elastic-plastic solids. *In* "Progress in Solid Mechanics" (I. N. Sneddon and R. Hill. eds.), Vol. 1, pp. 167–221. North-Holland, Amsterdam.

Koiter, W. T. (1964). Couple stresses in the theory of elasticity, I and II. *Proc. K. Ned. Akad. Wet. (B)* **67**(1), 17–44.

Kroner, E. (1958). "Kontinuumstheorie der versetzungen und eigenspannungen." Springer-Verlag, Berlin.

Kroner, E. (1961). Die neuen konzeptionen der kontinuumsmechanik der festen korper. *Physica Status Solidi* **1**, 3–16.

Kroner, E. (1962). Dislocations and continuum mechanics. *Appl. Mech. Rev.* **15**(8), 599–606.

Leroy, Y. M., and Molinari, A. (1993). Spatial patterns and size effects in shear zones: A hyperelastic model with higher-order gradients. *J. Mech. Phys. Solids* **41**(4), 631–663.

Lloyd, D. J. (1994). Particle reinforced aluminium and magnesium matrix composites. *Int. Mater. Rev.* **39**(1), 1–23.

Ma, Q., and Clarke, D. R. (1995). Size dependent hardness of solver single crystals. *J. Mater. Res.* **10**(4), 853–863.

Mclean, D. (1967). Dislocation contribution to the flow stress of polycrystalline iron. *Can. J. Phys.* **45**(2), 973–982.

Mindlin, R. D. (1963). Influence of couple-stresses on stress concentrations. *Exp. Mech.* **3**, 1–7.

Mindlin, R. D. (1964). Micro-structure in linear elasticity. *Arch. Ration. Mech. Anal.* **16**, 51–78.

Mindlin, R. D. (1965). Second gradient of strain and surface tension in linear elasticity. *Int. J. Solids Struct.* **1**, 417–438.

Muhlhaus, H. B. (1985). Oberflachen-Instabilitat bei geschichtetem halbraum mit biegesteifigkeit. *Ing. Arch.* **55**, 388–400 (in German).

Muhlhaus, H. B. (1989). Application of Cosserat theory in numerical solutions of limit load problems. *Ing. Arch.* **59**, 124–137.

Muhlhaus, H. B., and Aifantis, E. C. (1991). A variational principle for gradient plasticity. *Int. J. Solids Struct.* **28**(7), 845–857.

Needleman, A., Tvergaard, V., and Hutchinson, J. W. (1992). Void growth in plastic solids. *In* "Topics in Fracture and Fatigue" (A. S. Argon, ed.), pp. 145–178. Springer-Verlag, New York.

Nix, W. D. (1988). Mechanical properties of thin films. *Metall. Trans. A* **20A** 2217–2245.

Nye, J. F. (1953). Some geometrical relations in dislocated crystal. *Acta Metall.* **1**, 153–162.

Ponte Castenada, P. (1991). The effective mechanical properties of nonlinear isotropic composites. *J. Mech. Phys. Solids* **39**, 45–71.

Ponte Castenada, P. (1992). New variational principles in plasticity and their application to composite materials. *J. Mech. Phys. Solids* **40**, 1757–1788.

Poole, W. J., Ashby, M. F., and Fleck, N. A. (1996). Micro-hardness of annealed and work-hardened copper polycrystals. *Scripta Metall. Mater.* **34**(4), 559–564.

Rice, J. R., and Tracey, D. M. (1969). On the ductile enlargement of holes in triaxial stress fields. *J. Mech. Phys. Solids* **17**, 201–217.

Russell, K. C., and Ashby, M. F. (1970). Slip in aluminum crystals containing strong, plate-like particles. *Acta Metall.* **18**, 891–901.

Schiermeier, A. D., and Hutchinson, J. W. (1996). Crack tip fields in an elastic-plastic strain gradient solid in mode III. To be published.

Shu, J., and Fleck, N. A. (1996). Finite element analysis of micro-indentation—the role of length scale. *Int. J. Solids Struct.* submitted.

Sluys, L. J., de Borst, R., and Muhlhaus, H.-B. (1993). Wave propagation, localization and dispersion in a gradient-dependent medium. *Int. J. Solids Struct.* **30**(9), 1153–171.

Smyshlyaev, V. P., and Fleck, N. A. (1994), Bounds and estimates for linear composites with strain gradient effects. *J. Mech. Phys. Solids* **41**(12), 1851–1882.

Smyshlyaev, V. P., and Fleck, N. A. (1995). Bounds and estimates for the overall plastic behavior of composites with strain gradient effects. *Proc. R. Soc. London* **A451**, 795–810.

Smyshlyaev, V. P., and Fleck, N. A. (1996). The role of strain gradients in the grain size effect for polycrystals. *J. Mech. Phys. Solids* **44**, 465–496.

Steinmann, P. (1994). A micropolar theory of finite deformation and finite rotation multiplication elastoplasticity. *Int. J. Solids Struct.* **31**(8), 1063–1084.

Stelmashenko, N. A., Walls, M. G., Brown, L. M., and Milman, Y. V. (1993). Microindentations on W and Mo priented single crystals: An STM study. *Acta Metall. Mater.* **41**(10), 2855–2865.

Sternberg, E., and Muki, R. (1967). The effect of couple-stresses on the stress concentration around a crack. *Int. J. Solids Struct.* **3**, 69–95.

Sun, C. T., Achenback, J. D., and Hermann, G. (1968). Continuum theory for a laminated medium. *J. Appl. Mech.* **35**, 467–474.

Toupin, R. A. (1962). Elastic materials with couple stresses. *Arch. Ration. Mech. Anal.* **11**, 385–414.

Tvergaard, V. (1990). Material failure by void growth to coalescence. *Adv. Appl. Mech.* **27**, 83–147.

Xia, Z. C., and Hutchinson, J. W. (1996). Crack tip fields in strain gradient plasticity. *J. Mech. Phys. Solids* **44**, 1621–1648.

Zbib, H., and Aifantis, E. C. (1989). On the localization and postlocalization behavior of plastic deformation. Part I. On the initiation of shear-bands; Part II. On the evolution and thickness of shear bands. Part III. On the structure and velocity of Portevin-Le Chatelier bands. *Res. Mech.*, 261–277, 279–292, and 293–305.

Zuiker, J., and Dvorak, G. (1994). The effective properties of functionally graded composites-I. Extension of the Mori-Tanaka method to linearly varying fields. *Composites Engineering* **4**(1), 19–35.

Author Index

Numbers in italics refer to pages on which the complete references are cited.